FINAL REPORT

Project CG/DD/02

"Anthropogenic and biogenic influences on the oxidizing capacity of the atmosphere"

J.-F. Müller (Co-ordinator)
S. Wallens, M. Capouet
Institut d'Aéronomie Spatiale de Belgique
Avenue Circulaire 3, B-1180 Bruxelles

C. Vinckier (P.I)
V. Van den Bergh, I. Vanhees, F. Compernolle
Katholieke Universiteit Leuven
Department of Chemistry, Celestijnenlaan 200 F, B-3001 Heverlee-Leuven

Table of contents

ABSTRACT

The oxidizing capacity of the atmosphere determines the fate and lifetime of a large number of pollutants and greenhouse gases. It is affected by biogenic and anthropogenic emissions of chemical compounds, including hydrocarbons, carbon monoxide and the nitrogen oxides. In this project, the impact of these emissions on the formation of tropospheric ozone and other oxidants (including the hydroxyl radical OH) has been investigated through a combination of modelling activities and laboratory studies.

A first achievement of this project is the reduction of uncertainties in the chemical processes that determine the global distributions of tropospheric constituents. A number of chemical mechanisms, which have been identified to be potentially important, have been studied in the laboratory. More specifically, the products formed in the reaction of selected monoterpenes, in particular α-pinene and β-pinene, with hydroxyl radicals in the presence of an excess of oxygen have been identified and quantified. In order to achieve this goal, new analytical methods have been developed for the determination of both the volatile and semi-volatile reaction products. The study was carried out in a fast-flow reactor where hydroxyl radicals were generated from the reaction of hydrogen atoms with nitrogen dioxide. The reactor was equipped with a specially designed microwave cavity designed to operate at pressures up to 100 Torr. The volatile compounds were determined via on-line mass spectrometric analysis. In the case of the α-pinene, carbon dioxide, carbon monoxide, nitrogen dioxide and acetone were identified. The product yields were found to be pressure dependent, indicating that the fate of the initially formed α-pinene-OH adduct is determined by its stabilization rate. At low pressure of a few Torr, this adduct undergoes isomerization and decomposition reactions, while at a high pressure, it reacts mainly with molecular oxygen as is the case under atmospheric conditions. The semi-volatile products were collected on a liquid nitrogen trap and subsequently analyzed by GC-MS and HPLC-MS. When experiments were carried out at a total pressure of 50 Torr, GC-MS analysis showed that campholenealdehyde and pinonaldehyde were formed as oxidation products of the α-pinene/OH reaction, with pinonaldehyde being the main product. In the case of the β-pinene, nopinone is found to be the main oxidation product.

In addition, a new sampling method has been developed based on the conversion of aldehydes and ketones to 2,4-dinitrophenylhydrazone derivatives followed by HPLC-MS analysis. In this way formaldehyde, acetaldehyde and acetone could be determined. The quantification of the semi-volatile compounds was performed using two internal standards, benzaldehyde- and tolualdehyde-2,4-DNPH. Relative molar yields for the α-pinene/OH reaction products have been determined at 50 and 100 Torr, respectively: 9.7 ± 0.7 and 6 ± 5 for formaldehyde; 1.1 ± 0.1 and 0.9 ± 0.5 for acetaldehyde; 16 ± 1 and 6 ± 2 for acetone; 11 ± 2 and 5.5 ± 0.7 for campholenealdehyde; 63 ± 3 and 82 ± 7 for pinonaldehyde. For the reaction of β-pinene with hydroxyl radicals, the following products have been identified:

nopinone, acetone, acetaldehyde, formaldehyde, trans-3-hydroxynopinone, perillaldehyde, perilla alcohol and myrtanal.

A second achievement of this project is a better understanding of the processes controlling the abundance of tropospheric OH and a better quantification of the global budget of ozone and its precursors in the troposphere. Advances have been made towards a better quantification of ozone precursor emissions as well as a better quantification of their role in the global troposphere. For this latter purpose, two distinct chemical/transport models have been used. IMAGES, which provides global climatological distributions of chemical constituents, has been used to quantify the importance of many relevant processes (emissions, chemical reactions, etc.) on the global distribution and budget of tropospheric compounds. MOZART, which accounts for detailed meteorological variability, is most appropriate for the analysis of field observations. Note that, in spite of their different scopes, these models have similar formulations for chemical processes and emissions. In the framework of this project, these models have been intensively compared with chemical observations as well as with many other models. Numerical techniques have been developed to predict the impact of different sources on the distribution of ozone precursors (CO and NO_x). By this way, the pollutant emissions can be optimized in order to achieve a better agreement between the atmospheric model and the observations. The development of these inverse modelling techniques is an important step towards a better utilization of global measurements of pollutants such as the increasingly important satellite observations.

Among the ozone precursors, Biogenic Volatile Organic Compounds (BVOCs) have been given a special attention. Both their emissions by foliage and their subsequent fate in atmospheric conditions have been the subject of our investigations. A detailed BVOC emission model has been developed and tested against field measurements, in order to check the existing parameterizations. A chemical “box” model has been developed in order to integrate the existing knowledge on the oxidation of α-pinene (an important BVOC) by ozone, its largest oxidant. A gas/particle partitioning model has been included to allow the calculation of organic aerosol production from BVOC oxidation. Finally, the IMAGES model has been used in order to quantify the impact of hydrocarbons on the production of odd hydrogen (HO_x) and ozone in the upper troposphere. For example, the respective contributions of the photo-oxidation of acetone, aldehydes and hydroperoxides have been quantified and compared with the HO_x source due to ozone photolysis.

A third achievement of this project is the determination of the influence of human activities on the chemical composition and the oxidizing capacity of the atmosphere. IMAGES has been used to evaluate the impact of biomass burning and technological emissions, including aircraft emissions. Both past and possible future changes in the composition of the global troposphere have been the subject of our attention. In our estimations of the possible future (2050/2100) changes, the role of both the anthropogenic emissions increases (estimated from standard scenarios of economic and technological development) and water

vapor and temperature changes (estimated from a Global Circulation Model) were considered. Part of this work is a contribution to the recent 3rd IPCC Assessment Report.

1. INTRODUCTION

Several important threats for the global environment are currently being considered by the scientific community and by decision-makers. The depletion of stratospheric ozone has received much attention in the past and has triggered worldwide political action. A second global problem is the potential climate changes resulting from increasing emissions of greenhouse gases to the atmosphere. Although many uncertainties remain in the magnitude of these effects, climate conventions have been established calling for a reduction in the emissions. A third threat is the potential change in the global oxidizing capacity of the atmosphere. The importance of this question arises from the fact that pollution, which was regarded in the past as a local or regional problem, appears to affect the global atmosphere and could produce serious impacts on the Earth's biosphere (including humans) and on the climate system. The magnitude (and sometimes even the sign) of the effects remain uncertain and deserve detailed studies. An example of these problems is provided by the large increase recorded in the concentration of ozone in the atmospheric boundary layer over populated areas, and possibly also in remote areas. Changes may have occurred also in the free troposphere, but these are less documented. Ozone is an oxidant that can harm the productivity of crops and other plants and the health of humans. Ozone is also a greenhouse gas and, according to recent model calculations, could have contributed to 20% of the increase in the greenhouse forcing in the Northern Hemisphere since the pre-industrial era.

Another example is provided by the potentially important but unknown changes in the abundance of the hydroxyl radical (OH) in the troposphere. OH acts as a "detergent" of the atmosphere and, as such, determines the atmospheric lifetime of most chemical pollutants and of several greenhouse gases. Its concentration depends on the production of other gases including the nitrogen oxides (NO_x), CO, and hydrocarbons. Since no global measurement of OH is available, a study of OH and its past and future evolutions must involve a combination of experimental results and modelling studies.

Humans are perturbing the "chemical balance" of the atmosphere through changes in land-use, industrialisation and domestic activities. In certain cases, anthropogenic emissions have become larger than natural sources. Therefore, large impacts on the atmosphere are expected. Three-dimensional chemical-transport models (CTMs) of the atmosphere are thought to be the best tools in order to quantify the magnitude of these effects. *The determination of the influence of human activities on the chemical composition of the troposphere and on its oxidizing capacity is a major objective of this project.*

These impacts are difficult to estimate, though, due to the complexity of the chemical system, and also to the large uncertainties in several important processes. Among others: (a) the estimation of the global emissions of ozone precursors, in particular, CO, NO_x and non-methane hydrocarbons; (b) the chemistry of non-methane hydrocarbons; (c) the role of spatial and temporal variability; etc. It is therefore of critical importance (1) to perform extensive and detailed comparison of the model results with available observations of

atmospheric chemical compounds, as well as with other models, in order to identify the areas where the uncertainties are largest (this is best realised by the means of sensitivity studies); (2) to propose improved, more realistic parameterizations of the processes involved (emissions, chemical mechanism, sub-grid scale transport, numerical solving, etc.), based on the most recent and most advanced experimental and numerical studies. *The reduction of the uncertainties in the processes that determine the global distribution of chemical constituents (including oxidants) in the troposphere is a major objective of the present project.* This goal has been achieved by a combination of laboratory experiments and sensitivity studies using advanced models for the emissions, transport and chemical transformations of the ozone precursors.

Ozone precursors (hydrocarbons, CO and NO_x), which also influence OH, are partly produced by natural processes. For example, the largest source of volatile non-methane organic compounds (NMOCs) on the global scale is provided by the biogenic emissions of isoprene, terpenes and other species [Zimmermann et al. (1978), Müller (1992), Guenther et al. (1995)]. The emissions and photochemical degradation of these Biogenic Volatile Organic Compounds (BVOCs) in the atmosphere are a primary focus of the present project. Indeed, the uncertainty in the estimation of the global source of BVOC is thought to be a factor of 3. Isoprene being the single most important BVOC in terms of surface emissions, the verification of the isoprene emission algorithms by the means of comparisons with field observations is of particular importance and constitutes a specific focus of our project. The photochemical degradation of isoprene in the atmosphere, though, is believed to be well-known and is currently taken into account in many tropospheric CTMs. In contrast, the photooxidation of monoterpenes ($C_{10}H_{16}$) is much more complex and not well understood.

The monoterpenes can react with O_3 and radicals like OH and NO_3. Due to these reactions, these hydrocarbons have an influence on the concentrations of a number of trace gases in the atmosphere on a global scale [Warneck (1988)]. These trace gases include volatile compounds such as carbon monoxide and carbon dioxide [Hanst and Spence, (1980), Hatakeyama et al. (1991), Vinckier et al. (1998)], formaldehyde and acetone [Grosjean et al. (1992), Nozière et al. (1999)] and semi-volatile compounds like pinonaldehyde and nopinone [Hatakeyama et al. (1991), Nozière et al. (1999), Arey et al. (1990), Hakola et al. (1994)]. In addition, biogenic hydrocarbons are known to be involved in the production of atmospheric aerosols [Hatakeyama et al. (1991), Went (1960), Zhang et al. (1992), Hoffmann et al. (1997)].

Since the overall chemistry of BVOCs in the atmosphere is far too complex to study in situ, experiments have to be performed on a laboratory scale. To establish the degradation paths and to determine the product yields of the α/β-pinene/OH reactions, laboratory measurements can be carried out in smog chambers and fast-flow reactors. The disadvantage of smog chambers is the simultaneous occurrence of OH and O_3 reactions, whereas the fast-flow reactor technique has a clean OH-radical source. In this way the

reaction with hydroxyl radicals can be separated from other primary reactions with ozone or nitrate radicals.

Only rather recently, laboratory experiments have started to identify and quantify the reaction products of the terpene reactions. *A major objective of this project is to determine the products and the yields of the α-pinene and β-pinene reactions with hydroxyl radicals in the presence of an excess of molecular oxygen.* First, a sampling technique has been developed based on the capture and determination of these products on a liquid nitrogen trap. In the second part of the project, the reaction yields of the products have been determined quantitatively [Vanhees et al. (2001)].

2. MATERIALS AND METHODS

2.1. Fast-flow reactor

The fast-flow reactor technique with its clean OH-radical source was selected in order to simplify the reaction chemistry. Details of the experimental technique are given in references [Vinckier and Van Hoof, (1993), (1994)]. The fast-flow reactor consists of a quartz reactor with an internal diameter of 2.8 cm and a length of 70 cm. By means of an oil rotary pump with a nominal pump capacity of about 12 m^3 h^{-1}, a flow velocity of 3.81 m s^{-1} was obtained with helium as carrier gas. The time scale t_r of the reaction was determined by the position z of the axial inlet probe which is movable along the reactor axis and by the flow velocity v of the reagents : $t_r = z/v$. In these experiments z was set equal to 16 cm corresponding to a reaction time t_r of 42 ms.

The OH-radicals were generated by the titration reaction $H + NO_2 \rightarrow OH + NO$. The H-atoms needed for this reaction were produced by a microwave discharge in a H_2/He mixture. In all experiments the H_2-concentration was 1.37×10^{13} molecules cm^{-3} and the power of the discharge was 100 Watt (except for the blank where the discharge was turned off). In the past the microwave discharge technique, used to produce hydrogen atoms as precursors for the hydroxyl radicals, could only operate in a pressure range from 0.5 to 12 Torr (1 Torr = 133.322 Pa). This limitation was a major drawback of the fast-flow reactor technique since the results had to be extrapolated to much higher pressures to be relevant for atmospheric conditions. This problem has now been solved by installing a specially designed microwave cavity (type Surfatron) which allows to operate at pressures up to 100 Torr. The experiments were carried out at a total pressure of 50 or 100 Torr helium containing 20 % oxygen.

Hydroxyl radicals were produced in an upstream zone in the fast-flow reactor by allowing an excess of hydrogen atoms to react with NO_2 in a concentration of 3.62×10^{12} molecules cm^{-3}. In the downstream zone, addition of α/β-pinene is carried out by allowing a fraction of the carrier gas helium to flow through a vessel containing the α/β-pinene, resulting in a concentration of α/β-pinene in the reactor in the range from 10^{12} to 10^{13} molecules cm^{-3}. The amount of α/β-pinene consumed was determined by the weight difference before and after the experiments. At the downstream end, the quartz reactor was coupled directly to a mass spectrometer VG/MS/8-80 for qualitative and quantitative analysis of the volatile oxidation products.

2.2. Sampling method

The semi-volatile products were collected over a period of 5 to 6 hours on a liquid nitrogen (LN_2) trap and the batch samples were subsequently analysed by GC-MS and HPLC-MS. Two coating methods were used to collect these products : the LN_2 trap was coated with a frozen layer of dichloromethane (DCM) or with a layer of a 2,4-dinitrophenylhydrazine solution. The LN_2 trap is installed at the downstream end of the reactor.

2.2.1. LN_2 trap coated with DCM

The LN_2 trap can be coated with a layer of frozen DCM in the case of a qualitative analysis. At the end of a collection experiment, the trap is rinsed with about 50 ml DCM. After removal of the condensed water, the solution is concentrated by rotary evaporation at room temperature to about 1 ml. This remaining solution is further analyzed by GC-MS.

2.2.2. LN_2 trap coated with a 2,4-DNPH solution

In the second collection method used in the quantitative analysis, the trap was coated with a solution containing 2,4-dinitrophenylhydrazine (2,4-DNPH). The collection is based on the *in situ* conversion of aldehyde/ketone compounds to their 2,4-dinitrophenylhydrazone derivatives (see figure 1). This is the most frequently used method for the determination of carbonyls in ambient air [Grosjean et al, (1999), Yacoub (1999), Vairavamurthy (1992), Pötter and Karst, (1996), Grosjean and Grosjean, (1995), Grosjean (1983), Kölliker et al. (1998)]. Therefore, the stainless steel cold trap filled with liquid nitrogen was coated with a solution consisting of 2,4-dinitrophenylhydrazine (2,4-DNPH). The 2,4-DNPH solution was made by mixing 0.1 g of 2,4-DNPH with 0.7 ml diluted H_2SO_4.

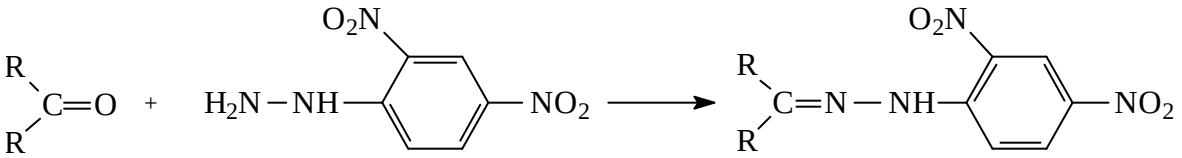

Aldehyde/ketone 2,4-dinitrophenylhydrazine 2,4-dinitrophenylhydrazone derivative

Figure 1: Reaction mechanism for the derivatization of aldehydes and ketones with 2,4-dinitrophenylhydrazine (in the presence of an acid) to form 2,4-dinitrophenylhydrazone derivatives.

The solution contains two internal standards: benzaldehyde-2,4-DNPH and tolualdehyde-2,4-DNPH. These two internal standards were needed because treating the trap could result in loss of the coating material. Benzaldehyde-2,4-DNPH was added to the coating solution prior to the coating of the LN_2 trap, whereas tolualdehyde-2,4-DNPH was added to the solution obtained after dissolving the collected residues from the LN_2 trap. Adding these two internal standards in the same concentration allows a correction for possible losses of the first internal standard benzaldehyde-2,4-DNPH. A solution containing benzaldehyde-2,4-DNPH and tolualdehyde-2,4-DNPH both in equal concentrations was analyzed by HPLC in order to derive the ratio of the two peak areas. The resulting value of 0.99 was used to check whether losses of benzaldehyde-2,4-DNPH and the coating occurred during collection experiments or not. Based on this value the loss of the first internal standard benzaldehyde-

2,4-DNPH could be calculated. In case the loss of benzaldehyde-2,4-DNPH occurred *after* the collection procedure, it was assumed that the products formed in the α/β-pinene/OH reaction were lost to the same extent. However, if during the coating of the LN_2 trap (*before* the collection experiment) some benzaldehyde-2,4-DNPH would be lost an "over" correction is performed.

2.3. Method of analysis

2.3.1. GC-MS

When the liquid nitrogen trap was coated with DCM, the evaporated solution was analyzed by GC-MS. The GC instrument Carlo-Erba (type Vega GC 6000) was equipped with a Chrompack CP-Sil 5 CB capillary column (25 m length x 0.33 mm inside diameter, df = 2.5 µm) and an on-column injection system. The flow of the helium carrier gas was ca. 1.5 ml min^{-1}. A quantity of 1-2 µl was injected on-column at an oven temperature of 60 °C. After elution of the solvent the oven temperature was raised at a rate of 8 °C min^{-1} to 200 °C. For all experiments electron impact (EI) spectra were recorded on a HP-5989A quadrupole mass spectrometer using an ion source temperature of 250 °C and an electron energy of 70 eV. The temperature of the interface between the GC and the MS was 180°C. The collected compounds were identified by comparing the GC-MS results with published GC-MS [Jay and Stieglitz, (1989)] and mass spectral data [Stenhagen and Abrahamsson, (1968)].

2.3.2. HPLC-MS

When the collection was based on the conversion of carbonyl compounds to their 2,4-dinitrophenylhydrazones, the carbonyl 2,4-DNPH-derivatives were analyzed using a HPLC-MS system equipped with Atmospheric Pressure Chemical Ionization (APCI; Micromass Quattro II). The negative ion mode was selected for the measurements [Kölliker et al. (1998)]. The scan range of the MS was from 150 to 600 for the determination of m/z values. The APCI probe temperature and the source temperature were 300°C and 80°C, respectively. The cone was set at 22 V. The 2,4-DNPH solutions were separated on a cc Nucleosil 100 C18 column (250 mm length x 3 mm inside diameter, 5 µm particles) using the Hewlett-Packard 1100 HPLC instrument. Separations were carried out at 35 °C using the following mobile phase gradient: from 5 % ACN / 95 % H_2O to 84 % ACN / 16% H_2O in 50 minutes followed by 10 min isocratic elution. The eluent flow rate was 0.6 ml/min and the sample volume injected was 10 µl using a Rheodyne injector. Both a diode array detector (DAD) and a mass spectrometer (MS) for Total Ion Current (TIC) were available as detector. The DAD was set at a wavelength of 360 nm. The mass spectrum corresponding to each peak in the TIC-chromatogram was compared with spectra of reference materials which were obtained from commercial sources or by synthesis.

2.4. Synthesis

2,4-DNPH derivatives of myrtanal, trans-3-hydroxynopinone, perillaldehyde, nopinone, campholenealdehyde and pinonaldehyde were synthesized according to the method described by Behforouz et al. (1985). From these products, only perillaldehyde and nopinone were commercially available. The other products were synthesized. Pinonaldehyde is synthesized by ozonolysis of α-pinene [Vinckier et al. (1997)]. Myrtanal is formed by a Swern oxidation on myrtanol [Peterson and Grant, (1991)]. Trans-3-hydroxynopinone is synthesized through ozonolysis of trans-pinocarveol which is formed by the reaction of α-pinene oxide with lithium diisopropylamide [Lavallée and Bouthillier, (1986)]. Reaction of α-pinene oxide with $ZnCl_2$ yielded campholenealdehyde [Vinckier et al. (1997)].

2.5. Reagents

The following reagents were supplied as gas mixtures : NO_2 (0.1 %) in helium (Oxhydrique), H_2 (0.1 %) in helium (Praxair), O_2 with a purity of 99.998 % (L'Air Liquide), He with a purity of 99.995 % (L'Air Liquide). The liquid reagents α- and β-pinene (Aldrich) had a purity of respectively 98 and 99 %. The solvents used were acetonitrile HPLC grade (Biosolve) and dichloromethane p.a. (Merck). 2,4-DNPH was recrystallized from ethanol, rinsed with ethanol and dried in a dessicator and analyzed by HPLC for possible carbonyl impurities. Formaldehyde-, acetaldehyde-, acetone-, benzaldehyde- and tolualdehyde-2,4-DNPH with a purity of 99 % were obtained from Supelco. Myrtanol (97 %, Aldrich), nopinone (98 %, Aldrich), perillaldehyde (99 %, Aldrich) and α-pineneoxide (97 %, Fluka) were commerically available.

2.6. Calibration solutions

For the quantitative measurements, calibration curves were constructed using the DAD as detector for the following components : formaldehyde-, acetaldehyde-, acetone-, campholenealdehyde-, and pinonaldehyde-di-2,4-DNPH. Benzaldehyde-2,4-DNPH was used as an internal standard.

2.7. The IMAGES model

IMAGES is a global, three-dimensional chemical transport model of the troposphere (Müller and Brasseur, 1995). It calculates the distribution of about 60 species, including ozone, odd hydrogen and odd nitrogen species, sulfur oxides (Pham et al. 1995; 1996), methane, non-methane hydrocarbons (ethane, propane, ethylene, propylene, acetone, isoprene, α-pinene, and n-butane as a surrogate for the other higher hydrocarbons) and their degradation products. Its horizontal resolution is 5° in latitude and in longitude. In the vertical the model includes 25 σ layers from the Earth's surface to the lower stratosphere (50 mbar). Large-scale transport is driven by monthly averaged winds (averaged over the period 1985-1989) taken from an analysis of the European Centre for Medium-Range Weather Forecasts

(ECMWF). The impact of wind variability at timescales smaller than one month is taken into account as a diffusion process, with diffusion coefficients estimated from the ECMWF wind variances, following the parameterization of Murgatroyd (1969). The water vapor distribution is also provided by the ECMWF analysis. Note that the use of the ECMWF analysis implies that the model should be considered as climatological, i.e., the modeled distributions do not represent any specific year, and inter-annual variations are ignored. Furthermore, the use of diffusion coefficients to represent temporal variability at short time scales implies that this model isn't appropriate to reproduce the chemical composition of the troposphere during particular episodes at short time scales. Therefore, the model results can't match the short-term variability in the chemical compounds as observed during field campaigns. Instead, the IMAGES model calculates "climatological " distributions of the most important tropospheric trace gases, i.e. multi-year averages in the 1980s and 1990s.

Vertical mixing in the planetary boundary layer is also represented as diffusion. The effect of deep convection on vertical transport is parameterized following Costen et al. (1988). The distribution of cloud updrafts is parameterized using the Cumulo-nimbus distribution estimated by the International Satellite Cloud Climatology Project (ISCPP) ("D2" climatology). In the latest versions of the model (Müller and Brasseur, 1999), convection and wet deposition schemes are modified to take rainout into account in the convective updrafts.

The trace gas emissions used in the model are those of Müller (1992) and Müller and Brasseur (1995), except that the GEIA (Global Emissions Inventory Activity) inventories are used in the latest versions for the fossil fuel emissions of NO_x and SO_x as well as for the biogenic emissions of BVOCs and NO_x.

2.8. The MOZART model

MOZART is a new three-dimensional global model based in part on the IMAGES model. Both models use the same chemical mechanism, photolysis rates, surface emissions, and dry deposition velocities. In contrast, the spatial resolution (T42 grid, i.e. about 2.8° in latitude and in longitude), the temporal resolution (time step of 20 minutes) and the representation of transport (semi-lagrangian transport from Rasch and Williamson (1990), convection and boundary layer transport parameterization taken from the NCAR Community Climate Model (CCM), a Global Circulation Model (GCM)) represent considerable improvements compared to IMAGES. The major drawback of these changes is the large computer costs they imply.

Dynamical variables (winds, convective fluxes, etc.) are updated every 3 hours. In a first version of the model (Brasseur et al., 1998; Hauglustaine et al., 1998), these fields were calculated off-line by the GCM. In a subsequent version of MOZART, meteorological fields are obtained from an analysis of observed (assimilated) winds taken from the European Centre for Medium-Range Weather Forecasts (ECMWF). In this case, the model calculates distributions of chemical species that are suitable for comparison with chemical data from measurement campaigns over specific periods of time. In both cases, and in contrast with the

IMAGES model, MOZART takes fully into account the temporal variability of dynamical fields as well as of photolysis frequencies (since the solar diurnal cycle and the time dependent impact of clouds are explicitly represented).

2.9. Comparisons with observations and with other models

By essence, models are oversimplified representations of reality. Furthermore, a large number of critical model parameters (e.g., chemical rate constants, pollutants emission fluxes, etc.) are poorly quantified. It is therefore of primary importance to evaluate the model performance by the means of extensive comparisons with observations of chemical species. Note that these measurements are generally also tainted with errors. And in some cases, data that are too sparse or too specific might lack representativity for model validation. The troposphere is indeed an extremely variable environment where some species mixing ratios might vary by orders of magnitude within short distances or short periods of time. The interpretation of model-data comparisons therefore requires caution.

The most convenient type of data traditionally used for model evaluation is represented by monthly averaged mixing ratios (averaged over several years) of slowly-varying compounds (O3, CO, CH4,...) at remote places. The year-to-year variations as well as the short-term high-frequency variations are filtered in these averages which can therefore be considered "climatological". Both IMAGES and MOZART have been extensively confronted with such data. These are represented by either surface mixing ratios or vertical profiles obtained by sondes on balloons (for ozone only) (Müller and Brasseur, 1995; Pham et al. 1995; Hauglustaine et al. 1998; Kanakidou et al. 1999a,b).

More recently, aircraft data have proved to be increasingly useful. For example, the routine ozone measurements performed by european commercial airliners in the framework of the MOZAIC program have provided an unprecedented climatology of upper tropospheric/lower stratospheric ozone concentrations over industrialized countries, the North Atlantic, and other regions (Law et al. 2000). Even more significant for model evaluation, dedicated aircraft campaigns (such as the NASA GTE missions and the european STRATOZ/TROPOZ campaigns) are of special interest. In these intensive campaigns, many different chemical compounds and meteorological parameters are measured simultaneously by a collection of sophisticated instruments onboard of aircraft flying in a specific region of particular interest for atmospheric scientists. Although the chemical distributions deduced from these campaigns cannot generally be considered as climatological, they provide unique insights on the role played by shorter-lived compounds such as the nitrogen oxides, oxygenated hydrocarbons, and even radicals. A broad compilation of observations taken from a majority of existing campaigns has been presented by Emmons et al. (2000), with detailed comparisons with the IMAGES and MOZART model distributions. An illustration is provided by the comparison of the measured and calculated vertical profiles of chemical species presented in Fig. 2. The observations reported here are those obtained during the american TRACE-A mission. The IMAGES and MOZART model results shown on the figure

were averaged over the mission area (here, Southern Africa). Differences between the two models are often important. They are due to differences in the transport scheme. In general, however, the models are seen to agree reasonably well with the observations. But IMAGES often predicts the existence of an unrealistic minimum in the concentrations of different compounds at around 4 km. This is directly related to the convection parameterization used in the model, which will be improved in future studies. Other comparisons with campaign data have been presented in Thakur et al. (1999), focusing on nitrogen compounds, and in Müller and Brasseur (1999), focusing on upper tropospheric precursors of odd hydrogen radicals.

In the future, remote sensing from space should provide an increasingly reliable and comprehensive set of chemical observations suitable for model validation and for scientific studies. In a preparative step towards this capability, the IMAGES model results have been used in order to optimize a CO/CH_4 retrieval algorithm for a satellite-based interferometer, IMG-ADEOS (Clerbaux et al., 1998). The modeled distribution of NO_2 have also been used to estimate the so-called air mass factors necessary to retrieve this compound by using satellite instruments like GOME (Lambert et al., 1999). The estimation of the tropospheric column of NO_2 by GOME onboard ERS2 (Lambert et al., 2000) and SCIAMACHY onboard ENVISAT will certainly prove to be of considerable help in order to understand the budget and distribution of nitrogen oxides in the troposphere.

In addition, the model outputs have also been compared with other models, in the framework of international intercomparison exercises (Friedl, 1997; Kanakidou et al. 1999a,b).

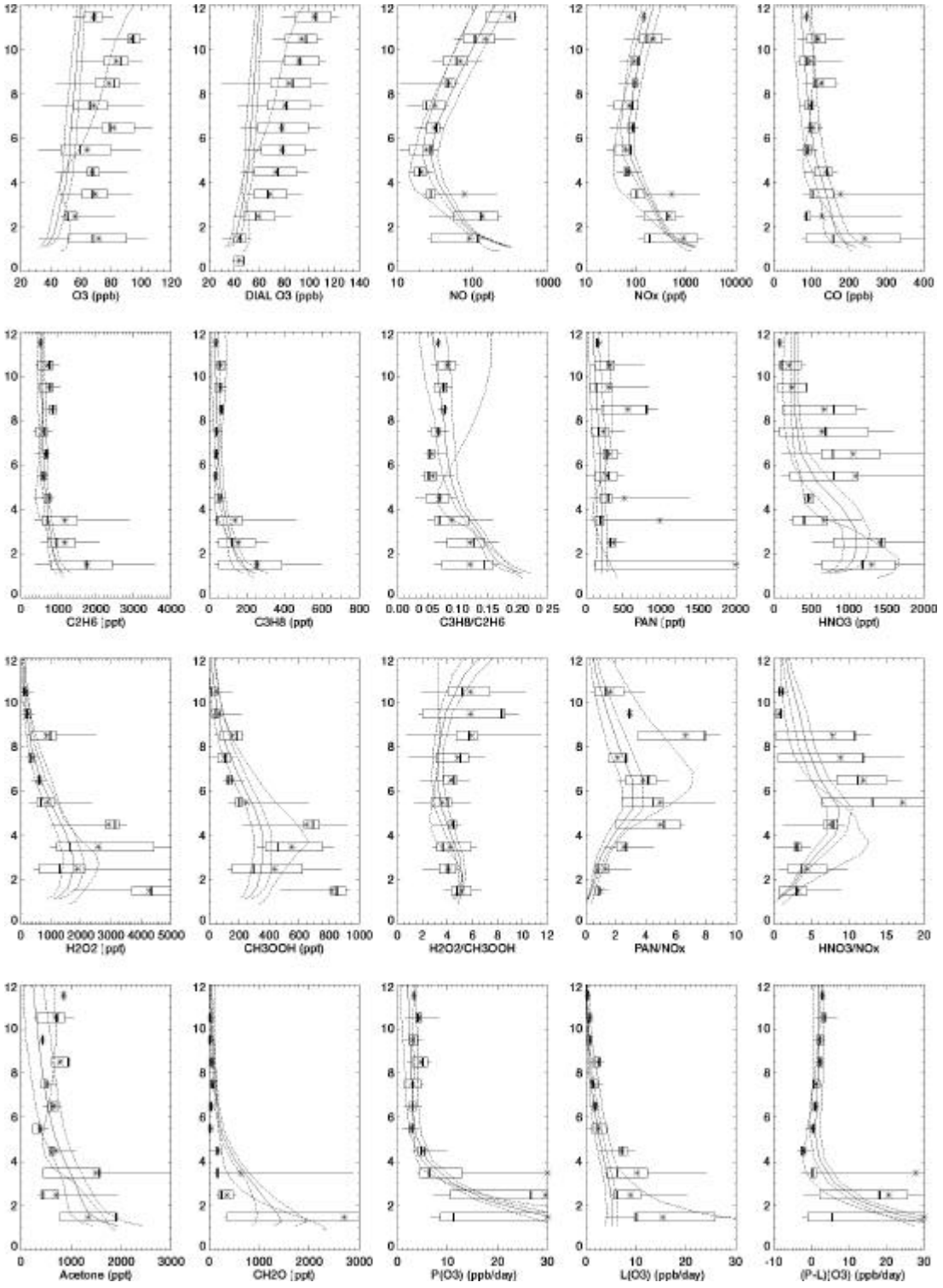

Figure 2. Vertical profiles of aircraft observations and IMAGES and MOZART results over Southern Africa during the TRACE-A campaign. Solid and dotted lines: MOZART mean and standard deviation in time; dashed lines: IMAGES. Boxes and whiskers indicate the central 50% and 90% of the observations, with a vertical bar at the median, a star at the mean. NO_x (=NO+NO_2) mixing ratio, as well as ozone production ($P(O_3)$), loss ($L(O_3)$) and net loss ($P-L)(O_3$) are estimated from a box model. Adapted from Emmons et al. (2000).

2.10. Estimating the source of odd hydrogen and ozone in the upper troposphere

The possibility that the subsonic aircraft fleet might enhance the levels of ozone in the upper troposphere/ lower stratosphere (UT/LS) has received considerable attention in the last years. Indeed, aircraft engines are known to release nitrogen oxides in the air, which are essential ingredients in the photochemical make-up of ozone in the troposphere. However, it is important to realize that this production of ozone is also strongly dependent on the levels of odd hydrogen, HO_x (=OH+HO_2). The main source of HO_x on the troposphere is the reaction sequence

$$O_3 + h\nu \rightarrow O_2 + O(^1D)$$
$$O(^1D) + H_2O \rightarrow 2\ OH$$

In the UT/LS, though, this production is impeded by the very low relative humidities particular to this region of the atmosphere. Other photochemical sources might therefore become important. We used the IMAGES model in order to calculate the relative contributions of the known photochemical sources to the total HO_x production in the UT/LS. It is believed that the an important source is represented by the convective transport of hydrogen peroxides, organic peroxides, and aldehydes from the Planetary Boundary Layer (PBL) to the UT/LS, followed by their photolysis or oxidation by OH. Therefore a tagging technique has been designed and used in the model in order to determine the role of convective transport on the UT/LS concentrations of these HOx precursors. Also, the precise yield of HO_x per (oxygenated) hydrocarbon oxidized or photolyzed has been calculated and shown to be a function of other compounds (NO_x in particular). In addition, the IMAGES model has been used in order to estimate the importance of these photochemical processes in the context of the perturbation represented by aircraft.

2.11. Modeling the emissions of biogenic volatile organic compounds (BVOCs)

As noted earlier, the emission of isoprene by terrestrial vegetation is known to provide the dominant input of reactive non-methane hydrocarbons to the atmosphere. Isoprene oxidation influences OH and ozone concentrations, has a significant role in CO production, the formation of organic acids, and photochemical conversion of NO_y species. Since isoprene can influence concentrations of ozone and gases that are removed by OH, including methane, isoprene emissions may indirectly impact climate.

The emissions of isoprene and other BVOCs, however, are still poorly quantified. A global inventory has been developed by Guenther et al. (1995) and is used by most tropospheric CTMs. This inventory relies on algorithms relating the emission rates to environmental factors and vegetation characteristics. BVOC emissions have been shown to depend on light intensity (Photosynthetically Active Radiation or PAR) and/or leaf temperature (Guenther et al., 1993, 1995):

$$F_1 = C_L\, C_{T1} \qquad (1) \qquad \text{(ex: isoprene, MBO)}$$

$$F_2 = \quad C_{T2} \qquad (2) \qquad \text{(ex: monoterpenes)}$$

Here, is a standard emission rate (emission rate at PAR=1000 µmol m^{-2} s^{-1}, and leaf temperature=30°C). This parameter depends on the compound being emitted and on the plant species. The factors C_L and C_{T1}, C_{T2} account for the dependence on PAR intensity and leaf temperature, respectively.

The validation of these algorithms by confrontation with field observations is necessary in order to quantify the possible biases and uncertainties in the global inventory, and also in order to check the impact of proposed model refinements. In that perspective, a detailed vegetation canopy microclimate model has been developed, in collaboration with the team of A. Guenther at NCAR. The fluxes of visible and infrared radiation inside the canopy are calculated from a multi-level (n=8 or 16) radiative transfer model. Leaf temperature in each layer is determined from the energy balance equation at the leaf level:

$$R_{sw} + R_{lw} + SH + LH = 0 \qquad (3)$$

where R_{sw}, R_{lw}, SH and LH are the solar radiation component, the thermal radiation component, the sensible heat flux and the latent heat flux, respectively. To solve this equation requires the determination of physical parameters such as boundary layer resistance to heat and water vapor, stomatal resistance, local wind speed, air temperature, relative humidity, etc. These parameters are related to leaf characteristics such as leaf dimension, leaf reflection coefficient, leaf emissivity, and canopy characteristics such as canopy height, LAI (Leaf Area Index), leaf biomass density, etc.

Figure 3 displays the comparison of isoprene fluxes measured and calculated by this model using the meteorological data (PAR, air temperature at canopy top) determined from the measurements. The site is located in a forest in Massachusetts. The isoprene fluxes were calculated with our model using either the leaf temperature or air temperature in equation (1). Modelled isoprene fluxes are found to be systematically underestimated compared with measurements when (eq. (1)) is deduced from vegetation composition and standard emission factors from the literature. We attribute this difference to an underestimation of either the standard emission factors used for oaks or the proportion of oaks (or other high-isoprene emitters) in the surrounding vegetation. It is also calculated that using air temperature (instead of leaf temperature) in equation (1) results in ~ 5 % higher emission estimates (average over the growing period). Sensitivity tests were performed showing that the isoprene emission estimates are not much influenced by possible errors in physical parameters such as the extinction coefficient, the leaf scattering coefficient, and the fraction of diffuse PAR.

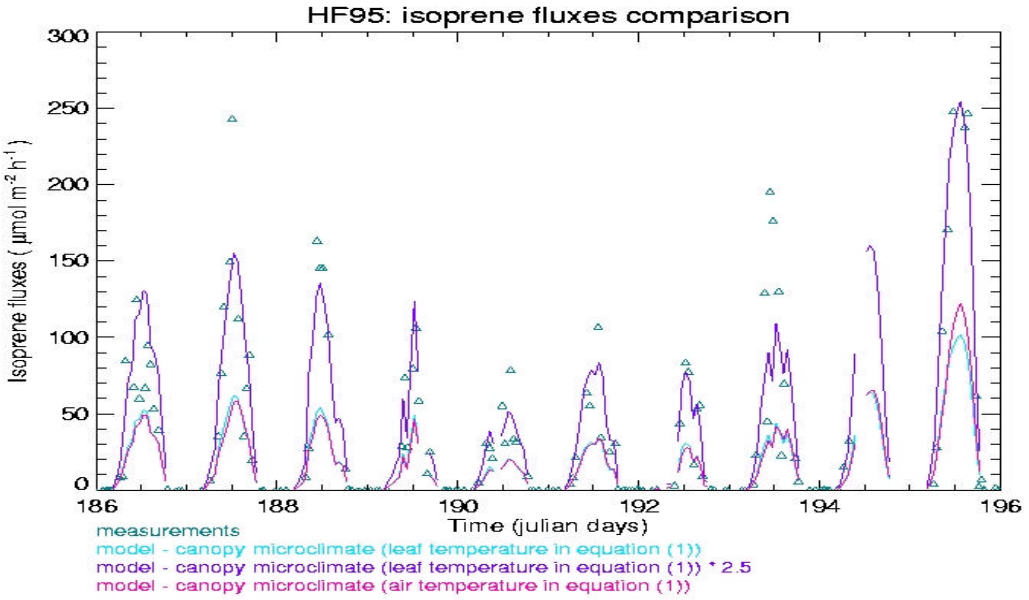

Figure 3. Isoprene emission fluxes measured and calculated at the Harvard forest site (see text for details).

2.12. Coloring techniques in the IMAGES model

The role played by the different emission sources (e.g., biomass burning, lightning, soils, etc.) on the distribution and budget of tropospheric pollutants can be investigated by variety of ways. The simplest method consists in varying the emission figures used in a chemical transport model (like IMAGES) and then comparing the results obtained in the different cases. It should be noted, however, that this is not equivalent to estimating the real relative contributions of the different sources on the tropospheric composition. Indeed, the residence time of a given tropospheric chemical species is generally a complex function of the geographical location, the time of the year, and the concentrations of many trace gases, including the compound of interest. This is especially true for carbon monoxide (CO) and nitrogen oxides (NO_x), since these important ozone precursors have a strong influence on the hydroxyl radical (OH) levels. The emissions of these gases are partly biogenic, and partly anthropogenic. In addition, CO is also one of the major end products in the atmospheric oxidation of methane and other hydrocarbons. This explains why it is so difficult to quantify the anthropogenic perturbation to the budget of important species.

In order to overcome these difficulties, innovative modelling techniques must be implemented. The "coloring" or "tagging" technique consists in assigning distinct "colors" or "flavors" to pollutant molecules emitted from different sources in an atmospheric CTM. This method allows to follow the evolution of any pollutant from any source without affecting the overall chemical state of the atmosphere. This technique has been first applied in IMAGES to study the relative contribution of different NO_x sources in the troposphere (Lamarque et al.,

1996). In this study, nitrogen originally emitted as one species (e.g., NO) is tagged so that it can be followed during all subsequent chemical transformations (e.g., to NO_2 and other products). If, for example, we consider only two sources, the total NO mixing ratio is written as NO=xNO + yNO, where xNO and yNO refer to the mixing ratio of NO associated with sources x and y, respectively. Six different sources were considered: aircraft, biomass burning, lightning, fossil fuel emissions, soils, and transport from the stratosphere.

In another study, the role of CO sources was investigated (Granier et al., 1999, 2000). This case is more complex because, in addition to surface emissions, the atmospheric oxidation of methane and non-methane hydrocarbons (NMHC) represents important sources of carbon monoxide. In order to distinguish between the contribution of methane, isoprene, terpenes and other hydrocarbons, a large number of oxygenated intermediates (e.g., CH_3O_2, CH_2O, PAN, etc.) involved in the oxidation mechanisms of these hydrocarbons must be "tagged" in order to follow the complete sequence of reactions between the initial hydrocarbon attack by OH, O_3, or $O(^1D)$ and leading eventually to CO. The surface emissions of carbon monoxide considered in our study include: technological sources, vegetation and ocean, biomass burning.

2.13. Inverse modelling of surface emissions of ozone precursors

The scientific exploitation of satellite-derived tropospheric columns of e.g. CO and NO_2 (two important ozone precursors in the troposphere) requires the development of new modelling techniques. Indeed, global distribution maps for these compounds are expected to provide useful insights on the distribution and strength of the emissions for these compounds. The pollutants emissions used in atmospheric models are based on various global emissions inventories (e.g. Müller, 1992) which are known to be very uncertain because of the major difficulty to extrapolate emissions estimates from local measurements to the global scale. In this perspective, the satellites should help to constrain the repartition of the total emissions into the different sources (e.g. anthropogenic, vegetation, ocean, etc.) and/or into different regions of the world. For that purpose, the pollutants emissions used in atmospheric models should be varied (roughly speaking, within their error bars) in order to minimize the biases between the modelled concentrations and the measurements. This general technique is commonly named inverse modelling.

In an exploratory study (Pétron et al., 2001), we restricted our objectives to the optimization of the surface emissions of CO on a monthly timescale, using monthly means of CO mixing ratio observations from the flask sampling network (CMDL) and the IMAGES model. The inversion scheme attempts to minimize the discrepancies between observed and modeled mixing ratios at the stations by optimizing the direct surface emissions of CO. In this approach, the transport model and the modeled chemical production of CO are assumed to have smaller uncertainties than CO surface emissions. It is also assumed that the relationship between the surface emissions and the concentrations at the measurement sites is linear. This assumption is shown to hold sufficiently well in this case, and a simple iterative

procedure is used in order to take the non-linearity into account to a good approximation. The numerical method adopted to perform the inversion (described in detail in Pétron et al. (2001)) is based on the tagging technique described in the previous section. In this study, 5 oceanic regions and 7 continental regions are considered. The continental surface emissions are due to technological activities, biomass burning (2 sub-categories: forest and savanna burning, agricultural waste burning and fuel wood use) and vegetation/microorganisms in soils. This brings a total of 33 tagged CO sources.

2.14. Development of a chemical box model for the oxidation mechanism of α-pinene

The oxidation of terpenes (α-pinene in particular) has received an increasing attention in the last years with a large number of laboratory and theoretical studies being conducted to identify the products and quantify the yields in various conditions. The laboratory investigation conducted in this project is an example of these studies. The extraordinary complexity of the terpene oxidation mechanism, however, makes the interpretation of experimental results extremely difficult. The laboratory conditions used (e.g., initial terpene concentration, NO_x levels, etc.) are most often very unrealistic and, even more significantly, they are generally not well controlled and understood. The partitioning of low-volatility products between the gas- and aerosol- phases represents an additional difficulty of crucial importance. This partitioning is thought to occur both in laboratory and atmospheric conditions, for compounds like the $C_{>9}$ acids and diacids, most (hydroxy) carbonyls, and most probably, for non-measured compounds like hydroperoxides and organic nitrates. The currently accepted gas/particle partitioning theory appears unable to account for the observations of the partitioning ratios for an important α-pinene degradation product, pinonaldehyde. Furthermore, the chemical pathways leading to the formation of highly condensable species like pinic acid (believed to play a crucial role in the aerosol formation process) are probably not understood. Much additional laboratory and theoretical investigations will be necessary in order to provide the kinetic data urgently needed by atmospheric models to estimate the role of terpenes in atmospheric chemistry.

For these reasons, we started the development of a chemical "box" model for the oxidation of α-pinene. The objective is to allow for a better interpretation of the existing laboratory data. Gas-phase chemical kinetic data on the α-pinene oxidation mechanism were provided by the team of J. Peeters at KULeuven on the basis of literature data and theoretical considerations. The resulting gas-phase chemical mechanism remains uncertain and is far from being complete, however. This work is in progress and will be continued in the framework of the OSTC's PADD2 (PODO2) program.

In addition to gas-phase chemical reaction, the partitioning of condensable species on aerosols is also considered, although nucleation of new particles and other microphysical processes are not described in detail. The partitioning coefficients of the condensables are estimated from the literature. This model has already been used to simulate a couple of published laboratory results for α-pinene ozonolysis. Our objective for the future will be the

implementation of a complete chemical mechanism and its validation and fine-tuning by the confrontation with a large number of existing laboratory data.

3. RESULTS

3.1. On-line mass spectrometric analysis of the volatile oxidation products of the α-pinene/OH reaction

The volatile products formed in the reaction between α-pinene and OH were determined quantitatively by measuring the signals of α-pinene, NO_2, CO_2, CO and acetone on-line by means of mass spectrometric detection [Vinckier et al. (1998)].

The product yield R is defined as the ratio of the concentration of the product formed to the amount of α-pinene reacted. The quantitative determination of the volatile products (CO_2 , CO, acetone and NO_2) was carried out at different total pressures with 20 % of the total pressure consisting of oxygen. The yields for CO_2, CO and acetone decreased when the pressure was increased, whereas the yield for NO_2 increased with pressure. The relation between pressure and the yields for the volatile components can be explained by considering the α-pinene-OH-adduct. This product is formed by addition of OH to the double bond in α-pinene. The adduct contains a large amount of internal energy and at low pressures it will isomerize or decompose to form several products including CO_2 , CO and acetone. At higher pressures the excited adduct is stabilized by collisions with a bath gas. Therefore, the amount of energy left will not be sufficient for decomposition to occur. There is not only the pressure effect of the higher helium concentration, but also the increase of the O_2 concentration at higher pressure, which is more efficient for the stabilization of the activated components [Vereecken and Peeters, (2000)].

3.2. Qualitative determination of the semi-volatile oxidation products for the α/β-pinene-OH reaction

3.2.1. α-pinene

As described in section 2.2.1., a first collection method consists of sampling the products on a LN_2 trap coated with dichloromethane. The reaction products collected on the cold wall were dissolved in DCM and then analysed by GC-MS. For each signal in the GC-MS chromatogram, the EI spectrum can be constructed and compared with reference data. When the experiments were carried out at pressures of 50 and 100 Torr, unreacted α-pinene, campholenealdehyde and pinonaldehyde were identified, with pinonaldehyde being the most important oxidation product. This is illustrated in Figure 4, where a GC-MS chromatogram is shown of the products found at 50 Torr. Similar results were obtained at 100 Torr (Van den Bergh et al. (2000)).

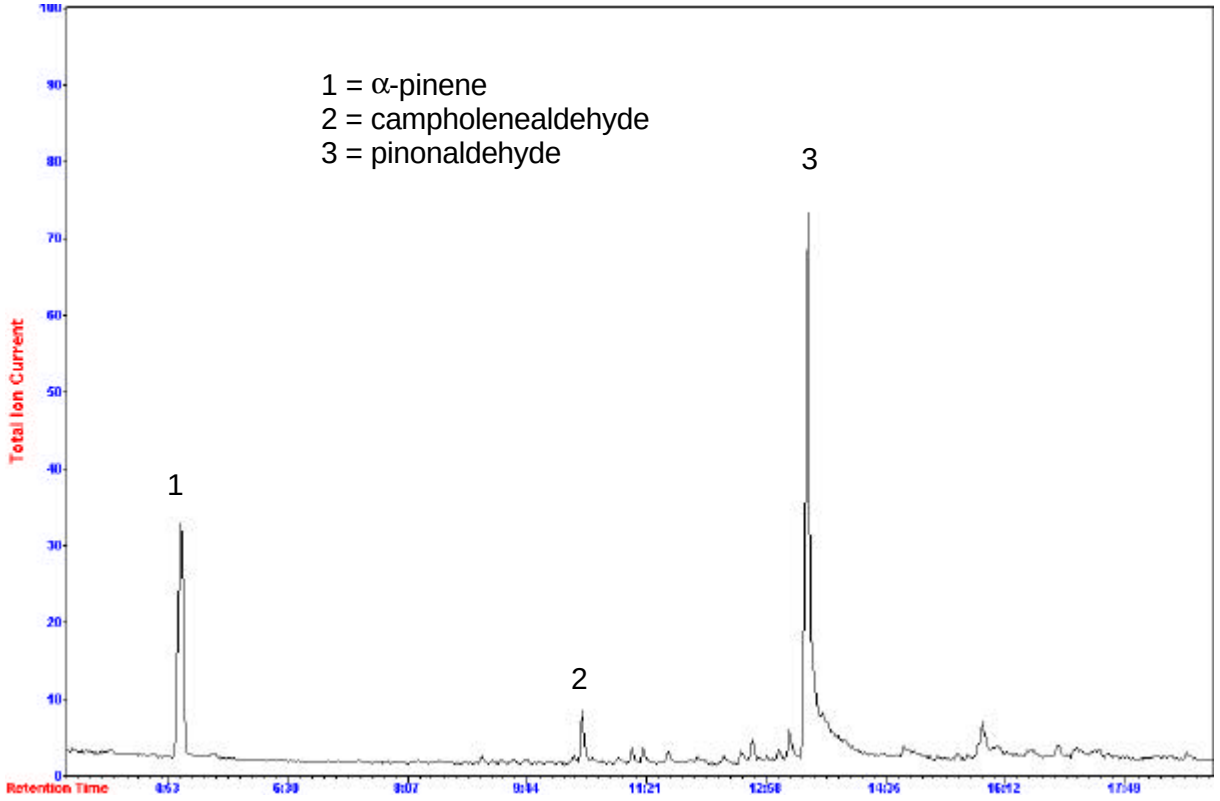

Figure 4 : GC-MS chromatogram of a collection experiment at a total pressure of 50 Torr. Initial concentrations : [α-$C_{10}H_{16}$] = 3.83×10^{12}, [H_2] = 1.37×10^{13}, [NO_2] = 3.63×10^{12}, [O_2] = 3.24×10^{17} each expressed in molec cm^{-3}. The reaction time t_r = 42 ms, collection time t_c = 381 min. Collection method: LN_2 trap coated with DCM.

A fundamental problem with this technique is to have a good method for collecting semi-volatile components from a high velocity gas stream passing through a LN_2 trap at low pressure. The semi-volatile products like formaldehyde, acetaldehyde and acetone are not detected when DCM is used as collection agent. Although these products can be captured on the LN_2 trap they are lost while evaporating the solvent. This rotary evaporation was required to reduce the solution from approximately 50 ml to 2-3 ml prior to GC injection. Therefore another coating procedure is developed.

The new method is based on the conversion of the aldehydes/ketones to 2,4-dinitrophenylhydrazone derivatives. The aldehydes and ketones formed in the oxidation reaction of α-pinene were collected on the LN_2 trap coated with a solution of 2,4-DNPH in ACN-DCM containing benzaldehyde-2,4-DNPH as the first internal standard. A quantitative transfer to the cold LN_2 trap was facilitated by instantaneous freezing out of consecutive layers of the ACN-DCM solution applied to the inner wall of the trap. At the end of the collection experiment, the reaction products collected on the cold wall were recovered by rinsing the frozen solution with further portions of ACN-DCM solvent mixture, followed by addition of tolualdehyde-2,4-DNPH. This solution containing the two internal standards was further analyzed by HPLC-MS. First a blank experiment was run in the absence of α-pinene and OH radicals. The resulting HPLC chromatogram in figure 5 shows that besides 2,4-DNPH, only the signals of the two internal standard were observed.

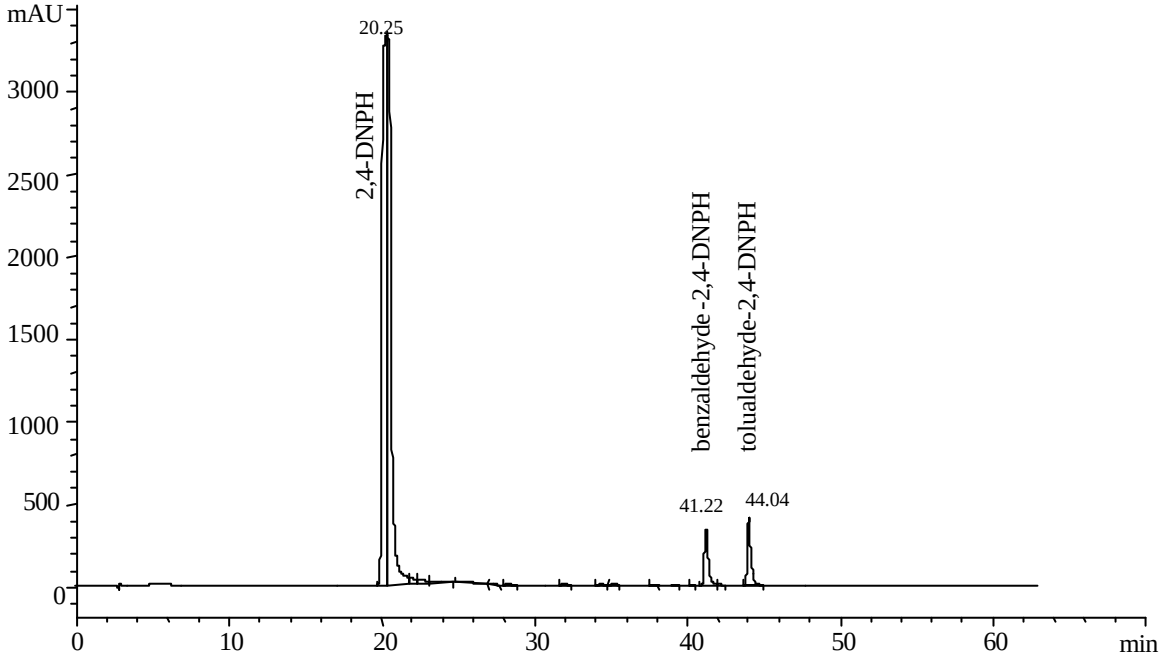

Figure 5 : HPLC (DAD, 360 nm) chromatogram (blank collection experiment) at a total pressure of 50 Torr. Initial concentrations : [α-$C_{10}H_{16}$] = 0, [H_2] = 1.37x10^{13}, [NO_2] = 0, [O_2] = 3.24x10^{17} each expressed in molec cm^{-3}. Microwave discharge turned off. The reaction time t_r = 42 ms, collection time t_c = 170 min.

When α-pinene was reacting with OH radicals at 50 Torr pinonaldehyde-di-2,4-DNPH (t_R= 51.1 min, M_r = 528) was identified as the main product. Other identified products shown in figure 6 are campholenealdehyde-2,4-DNPH (t_R = 49.4 min, M_r = 332), formaldehyde-2,4-DNPH (t_R = 28.7 min, M_r = 210), acetaldehyde-2,4-DNPH (t_R = 32.2. min, M_r = 224) and acetone-2,4-DNPH (t_R = 35.4 min, M_r = 238). Besides these oxidation products, the chromatogram shown in figure 6 contains three other peaks : dinitroaniline (t_R = 22.5 min) and two unidentified products with t_R = 25.1 min and t_R = 27.0 min. Because the same peaks are detected in a blank experiment with OH radicals but in the absence of α-pinene, it is clear that these products do not result from the α-pinene/OH reaction.

The oxidation products could be identified according to their retention times observed in the Total Ion Chromatogram (TIC) (not shown here). The mass spectrum of each peak can be constructed from the TIC and compared with mass spectral data of reference compounds. The mass spectra of the reference compounds obtained from commercial sources or by synthesis are shown in figure 7. A summary of the retention times, identified products, $(M-H)^-$ values and molecular masses is presented in Table 1.

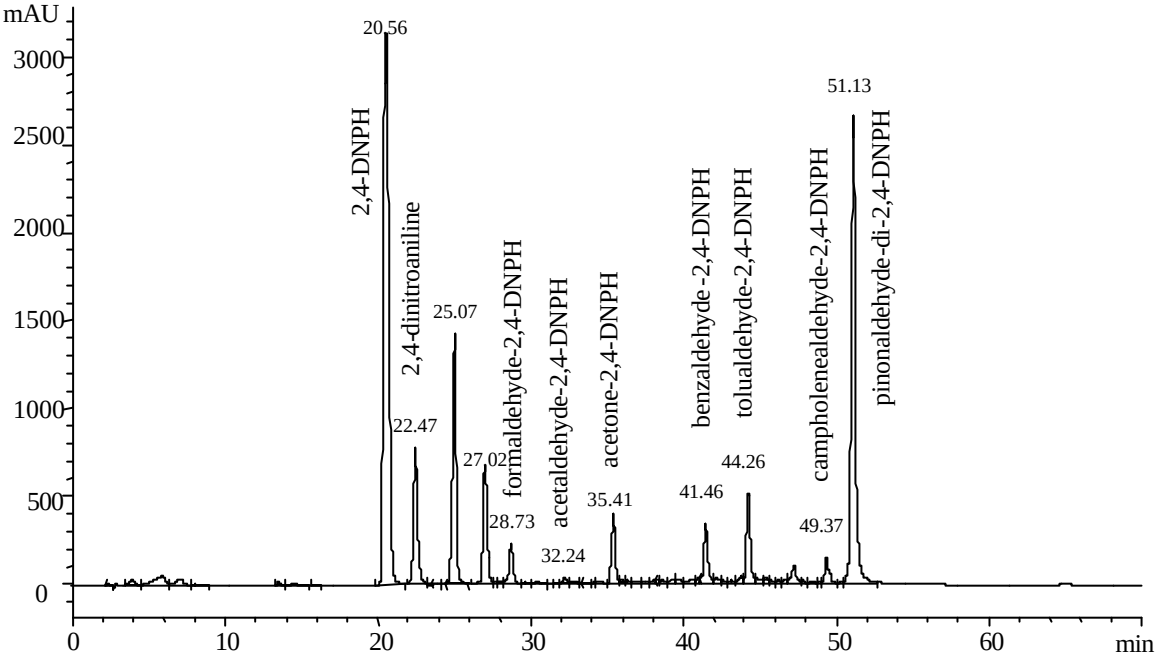

Figure 6 : HPLC (DAD, 360 nm) chromatogram at a total pressure of 50 Torr. Initial concentrations : $[\alpha\text{-}C_{10}H_{16}] = 5.08\text{x}10^{12}$, $[H_2] = 1.37\text{x}10^{13}$, $[NO_2] = 3.62\text{x}10^{12}$, $[O_2] = 3.24\text{x}10^{17}$ each expressed in molec cm^{-3}. The reaction time t_r = 42 ms, collection time t_c = 306 min. Collection method : LN_2 trap coated with 2,4-DNPH solution.

Table 1. Retention times t_R, $(M-H)^-$ values and molecular masses M_r of the identified products

t_R (min)	product	$(M-H)^-$	M_r
19.3	2,4-DNPH	197	198
27.2	formaldehyde-2,4-DNPH	209	210
30.9	acetaldehyde-2,4-DNPH	223	224
33.9	acetone-2,4-DNPH	237	238
38.2	pinonaldehyde-mono-2,4-DNPH	347	348
48.8	campholenealdehyde-2,4-DNPH	331	332
50.0	pinonaldehyde-di-2,4-DNPH	527	528

3.2.2. β-pinene

An analogous study has been performed on the β-pinene/OH reaction. The resulting GC-MS chromatogram for a collection experiment performed at a total pressure of 50 Torr and with the trap coated with DCM, is shown in figure 8. Nopinone is the main oxidation product. Besides nopinone, small signals can be observed which were attributed to myrtanal, trans-3-hydroxynopinone, perillaldehyde and perilla alcohol. Similar results have been obtained for experiments performed at 100 Torr [Van den Bergh et al. (2001)].

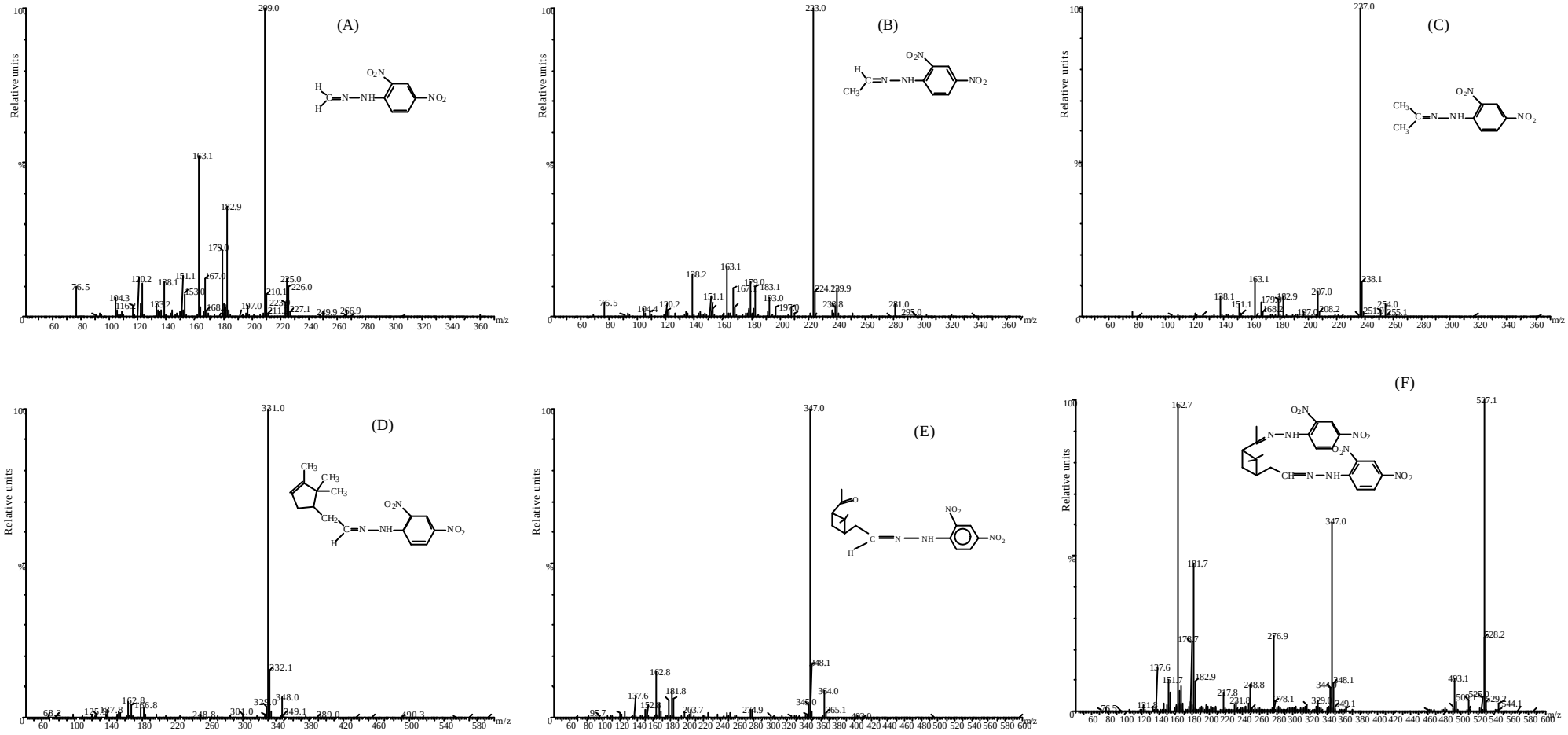

Figure 7 : APCI(-) generated mass spectra of reference materials obtained from commercial sources [(A) formaldehyde-2,4-DNPH, (B) acetaldehyde-2,4-DNPH, (C) acetone-2,4-DNPH] or by synthesis [(D) campholenealdehyde-2,4-DNPH, (E) pinonaldehyde-mono-2,4-DNPH and (F) pinonaldehyde-di-2,4-DNPH)]

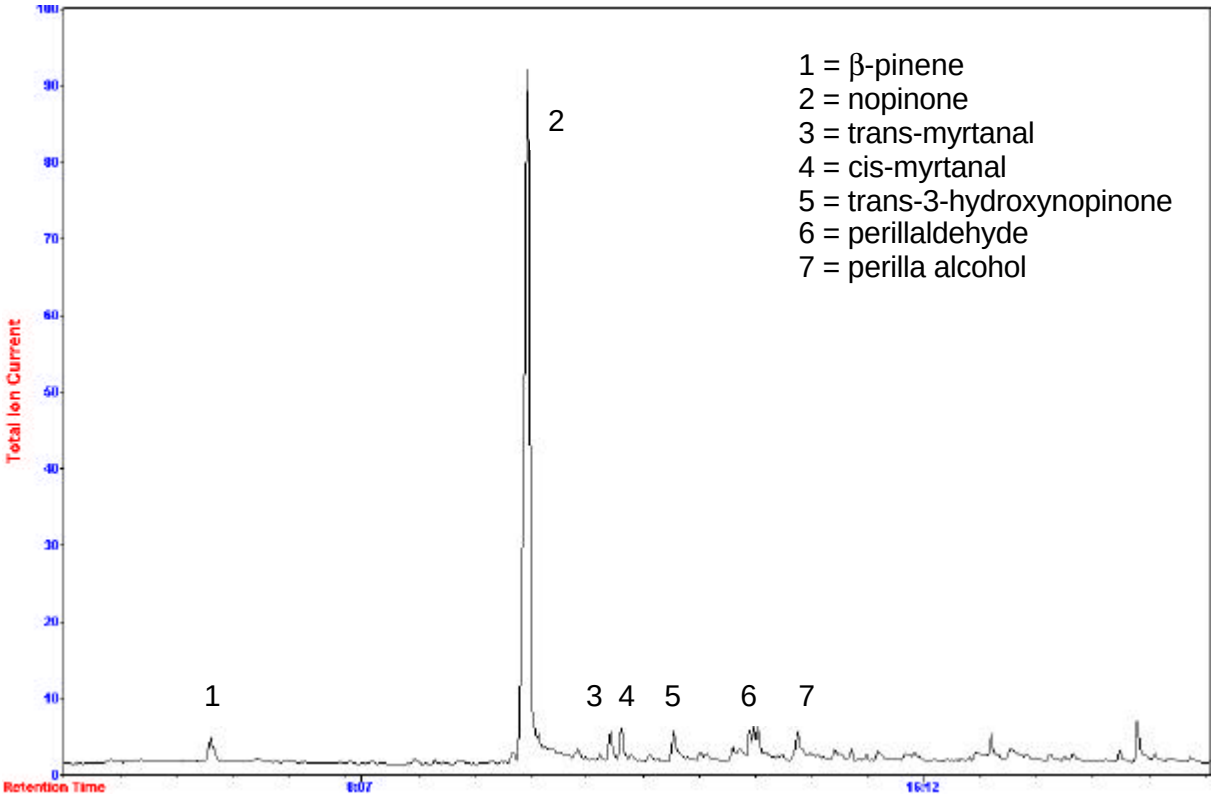

Figure 8 : GC-MS chromatogram of a collection experiment at a total pressure of 50 Torr. Initial concentrations : [β-$C_{10}H_{16}$] = 4.81×10^{12}, [H_2] = 1.37×10^{13}, [NO_2] = 3.63×10^{12}, [O_2] = 3.24×10^{17} each expressed in molec cm^{-3}. The reaction time t_r = 42 ms, collection time t_c = 437 min. Collection method : LN_2 trap coated with DCM.

Using the collection method, where the LN_2 trap is coated with a 2,4-DNPH solution the products shown in figure 9 were identified. The identified oxidation products, retention times, (M-H) values and molecular masses are summarized in table 2. The mass spectral data of the reference compounds nopinone-, trans-3-hydroxynopinone-, perillaldehyde- and myrtanal-2,4-DNPH are shown in figure 10.

Table 2 : Retention times t_R, $(M-H)^-$ values and molecular masses M_r of the identified products for the β-pinene/OH reaction

t_R (min)	product	$(M-H)^-$	M_r
20.1	2,4-DNPH	197	198
28.3	formaldehyde-2,4-DNPH	209	210
31.8	acetaldehyde-2,4-DNPH	223	224
34.9	acetone-2,4-DNPH	237	238
38.7	trans-3-hydroxynopinone-2,4-DNPH	333	334
46.4	nopinone-2,4-DNPH	317	318
49.6	perillaldehyde-2,4-DNPH	329	330
49.9	myrtanal-2,4-DNPH	331	332

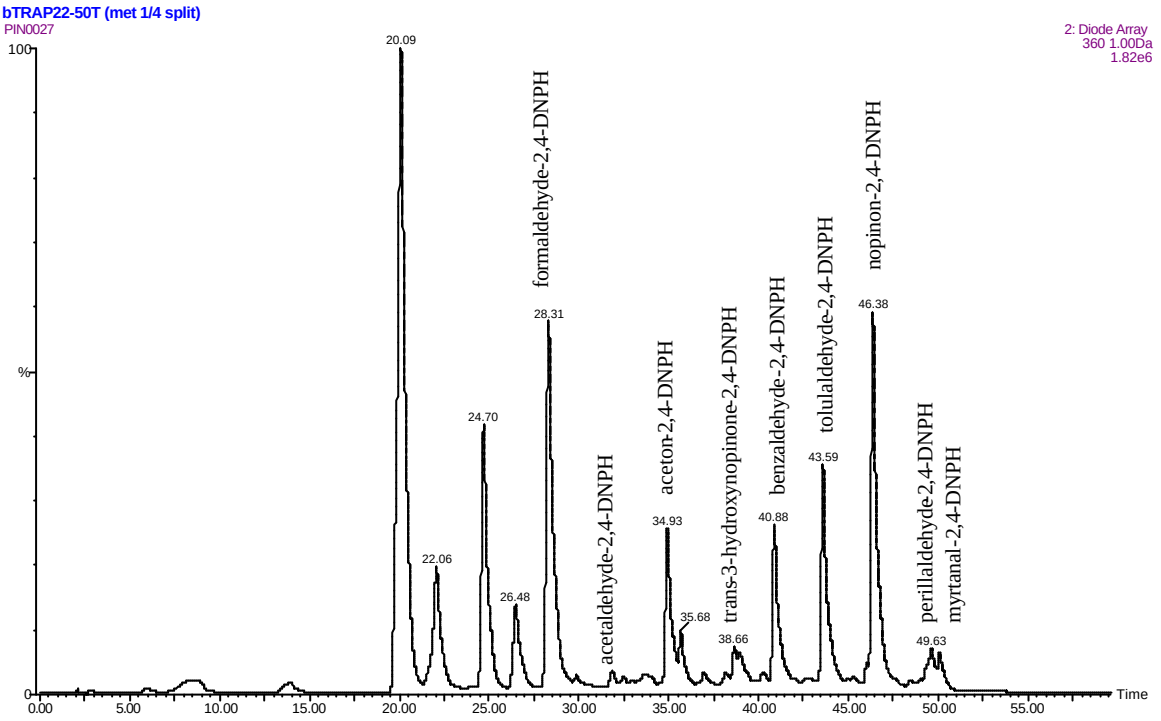

Figure 9 : HPLC (DAD, 360 nm) chromatogram at a total pressure of 50 Torr. Initial concentrations : [α-$C_{10}H_{16}$] = 5.08x10^{12}, [H_2] = 1.37x10^{13}, [NO_2] = 3.62x10^{12}, [O_2] = 3.24x10^{17} each expressed in molec cm^{-3}. The reaction time t_r = 42 ms, collection time t_c = 306 min. Collection method : LN_2 trap coated with 2,4-DNPH solution.

3.3. Quantitative determination of the semi-volatile oxidation products for the a-pinene-OH reaction

3.3.1. Product yields at 50 and 100 Torr

For quantitative measurements the LN_2 trap is coated with a 2,4-DNPH according to the procedure described in section 2.2.2.. The standard solutions described in section 2.6. were used to construct calibration curves for formaldehyde-, acetaldehyde-, acetone-, campholenealdehyde- and pinonaldehyde-di-2,4-DNPH with benzaldehyde-2,4-DNPH as an internal standard. A detailed description of the quantitative determination of the product yields is given in Vanhees et al. (2001). The mean value of the product yields for the five oxidation products at 50 and 100 Torr are shown in table 3. Assuming the same collection efficiency on the LN_2 trap, one can conclude that pinonaldehyde is the most abundant semi-volatile oxidation product, present for 63 mol % at 50 Torr and about 82 mol % at 100 Torr.

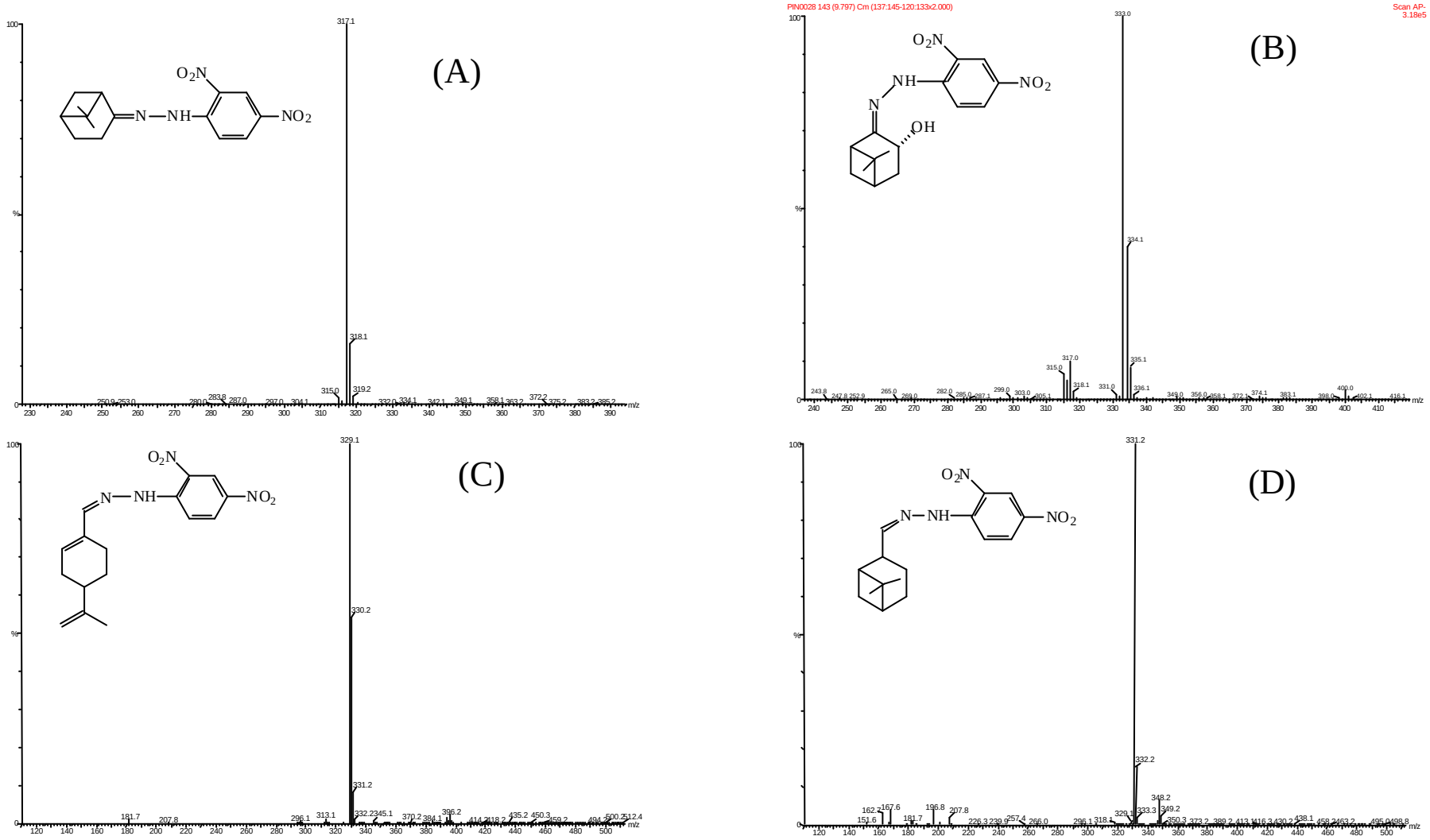

Figure 10 : APCI(-) generated mass spectra of reference materials obtained by synthesis [(A) nopinone-2,4-DNPH, (B) trans-3-hydroxynopinone-2,4-DNPH, (C) perillaldehyde-2,4-DNPH] and (D) myrtanal-2,4-DNPH]

Table 3 : Product yields expressed in relative units of the five oxidation products at 50 and 100 Torr. Experimental conditions: [α-$C_{10}H_{16}$] ~ $5x10^{12}$, [H_2] = $1.37x10^{13}$, [NO_2] = $3.62x10^{12}$, [O_2] = $3.24x10^{17}$ (50 Torr), [O_2] = $6.48x10^{17}$ (100 Torr) each expressed in molec cm^{-3}. The reaction time t_r = 42 ms.

	Relative amount (mol %)	
	50 Torr	**100 Torr**
formaldehyde	9.7 ± 0.7	6 ± 5
acetaldehyde	1.1 ± 0.1	0.9 ± 0.5
acetone	16 ± 1	6 ± 2
campholenealdehyde	11 ± 2	5.5 ± 0.7
pinonaldehyde	63 ± 3	82 ± 8

3.3.2. Influence of NO

The relative product yields shown in table 4 for an extra added NO concentration of $1.67x10^{13}$ molec cm^{-3} are maximum values for formaldehyde, acetaldehyde, acetone and campholenealdehyde and minimum values for pinonaldehyde. This is due to the fact that also pinonaldehyde-mono-2,4-DNPH was detected. Taking this information into account, it can be concluded that adding extra NO to the system has no pronounced effect on the relative product yields. The yields of acetaldehyde and campholenealdehyde slightly decrease.

Table 4. Product yields of the five oxidation products in relative units. Experimental conditions: [O_2] = $3.24x10^{17}$ (50 Torr), [H_2] = $1.37x10^{13}$, [NO_2] = $3.62x10^{12}$, [α-pinene] ~ $5x10^{12}$ (expressed in molec. cm^{-3}), t_r = 42 ms.

$[NO]_{extra}$ (molec cm^{-3})	0	$1.67x10^{13}$
formaldehyde	9.7 ± 0.7	14.4
acetaldehyde	1.1 ± 0.1	0.8
acetone	16 ± 1	20.8
campholenealdehyde	11 ± 2	8.3
pinonaldehyde	63 ± 3	55.7

3.3.3. Influence of the reaction time

The results in table 5 show that the axial distance z and the reaction time t have no systematic effect on the relative product yields at reaction times longer than 42 ms. This indicates that subsequent reactions of the carbonyl compounds are unimportant in our experimental conditions.

Table 5: Product yields for the five oxidation products in relative units at different reaction times t_r. Experimental conditions: $[O_2]$ = 3.24x10^{17} (50 Torr), $[H_2]$ = 1.37x10^{13}, $[NO_2]$ = 3.62x10^{12}, [α-pinene] ~ 5x10^{12} (expressed in molec cm^{-3}).

z (cm)	16	26	31	36	41
t_r (ms)	42	68	81	94	108
formaldehyde	9.7 ± 0.7	8.7	10.9	11.0	13.5
acetaldehyde	1.1 ± 0.1	0.7	1.3	1.1	1.7
acetone	16 ± 1	19.2	17.4	16.8	19.9
campholenealdehyde	11 ± 2	6.9	9.8	7.5	8.5
pinonaldehyde	63 ± 3	64.5	60.6	63.6	56.3

3.3.4. Influence of the initial H_2-concentration

The results shown in table 6 indicate that doubling of the initial H_2-concentration has no systematic effect on the relative product yields.

Table 6 : Product yields for the five oxidation products in relative units at different initial [H]. Experimental conditions: $[O_2]$ = 3.24x10^{17} (50 Torr), $[NO_2]$ = 3.62x10^{12}, [α-pinene] ~ 5x10^{12} (expressed in molec cm^{-3}), t_r = 42 ms.

$[NO_2]$ (molec cm^{-3})	3.62x10^{12}	
$[H_2]$ (molec cm^{-3})	1.38x10^{13}	6.91x10^{12}
formaldehyde	9.7 ± 0.7	8 ± 2
acetaldehyde	1.1 ± 0.1	0.8 ± 0.5
acetone	16 ± 1	13 ± 3
campholenealdehyde	11 ± 2	9.8 ± 0.4
pinonaldehyde	63 ± 3	68 ± 6

3.4. Discussion and interpretation of laboratory results for α-pinene

From the qualitative and quantitative analysis described above, the following products were formed in the α-pinene/OH reaction in the presence of oxygen and nitric oxide : formaldehyde, acetaldehyde, acetone, campholenealdehyde and pinonaldehyde.

A reaction mechanism leading to the formation of formaldehyde, acetone, campholenealdehyde and pinonaldehyde is illustrated in figure 11. In a first step an OH-radical is added to α-pinene. The α-pinene/OH-adduct can either react directly with O_2

(**A**) or isomerize (**B**, **C**). The reaction with O_2 (**A**), followed by O-abstraction with NO, results in a α-pinene/OH/O-adduct. Next, one pathway (**D**) leads to the formation of formaldehyde and another one (**E**) including an H-abstraction with molecular oxygen, leads to the formation of pinonaldehyde. The isomers of the α-pinene/OH-adduct can either lead to the formation of campholenealdehyde (**B**) or react with O_2 and NO, resulting in the formation of acetone (**C**).

For acetaldehyde, which has not been identified before as an oxidation product, the mechanisms shown in Figure 12 are proposed. First, acetaldehyde can be formed by tautomerisation of vinylalcohol in an acidic solution. Vinylalcohol could arise as the initial gas-phase product via decomposition of radical X or Y **(A)**. Because this tautomerisation reaction occurs in solution it is not possible to conclude whether or not acetaldehyde is formed as an oxidation product of the α-pinene/OH reaction in the gas phase. However, if acetaldehyde were to be a real gas phase oxidation product, scheme **B** in Figure 12 is a possible pathway. Formaldehyde and acetone were also identified in a smog chamber study by Grosjean et al. (1992), who used cartridges impregnated with 2,4-DNPH followed by HPLC-MS (CI) detection. Nozière et al. (1999) also detected these products but here Fourier Transform InfraRed (FTIR) was used. The presence of pinonaldehyde was demonstrated by several techniques: GC-MS and GC-FTIR [Hakola et al. (1994)], GC-MS and GC-FID [Arey et al. (1990)], and FTIR [Hatakeyama et al. (1991), Nozière et al. (1999)]. Up till now acetaldehyde and campholenealdehyde have not been identified as products of the α-pinene/OH reaction under atmospheric conditions.
Several mechanisms were proposed in the literature [Nozière et al. (1999), Pilling et al. (1999), Atkinson and Arey, (1998), Fantechi (1999)]. One of the first publications in which reaction schemes were elaborated explaining the formation of the majority of the semi-volatile compounds is given in Vinckier et al. (1997). The reaction pathways for formaldehyde and pinonaldehyde are similar to the mechanisms proposed by Nozière et al. (1999). It should be pointed out though that the reaction schemes don't take into account initial hydrogen abstraction reactions by the OH-radical from α-pinene [Atkinson and Arey, (1998), Fantechi (1999)]. If that path would be important, other reaction channels may open up leading to the formation of the observed products.

At 50 Torr, the product yields of the five oxidation products in relative units (mole %) are : formaldehyde (9.7 ± 0.7), acetaldehyde (1.1 ± 0.1), acetone (16 ± 1), campholenealdehyde (11 ± 2) and pinonaldehyde (63 ± 3). The yields at 100 Torr are (in mole %) : formaldehyde (6 ± 5), acetaldehyde (0.9 ± 0.5), acetone (6 ± 2), campholenealdehyde (5.5 ± 0.7) and pinonaldehyde (82 ± 7). The results clearly indicate that at 50 and 100 Torr pinonaldehyde is the main reaction product. In comparison with the results at 50 Torr, the yield of pinonaldehyde is higher at 100 Torr, while the yields of the other products, especially acetone and campholenealdehyde, decrease. A possible explanation for this pressure dependence can be derived from the reaction mechanism proposed in figure 11. Assuming that the initially formed α-pinene-OH adduct is more readily stabilized at higher pressure, less isomerization occurs leading to a lower formation rate of acetone and campholenealdehyde.

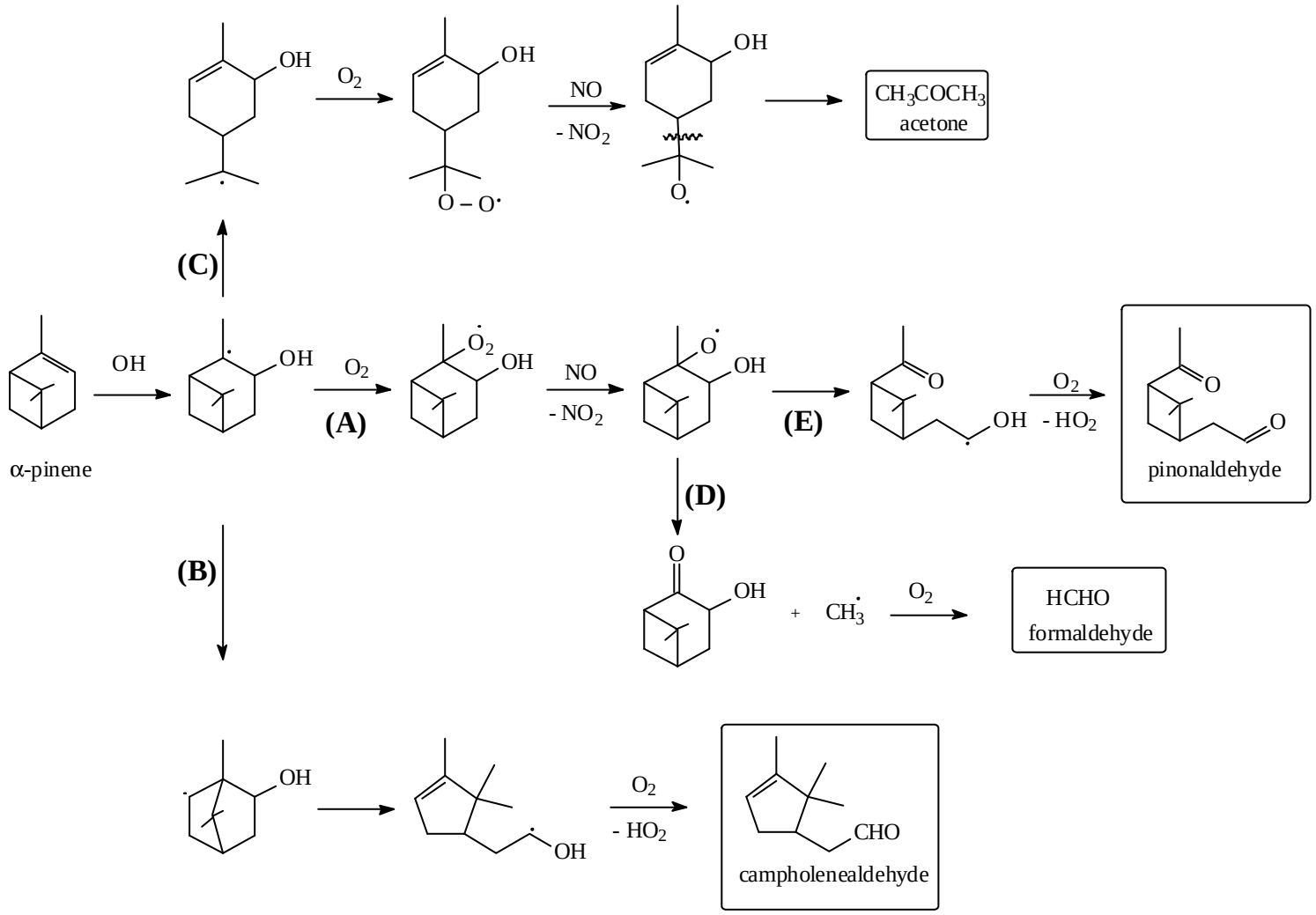

Figure 11: Mechanism for the reaction between α-pinene and OH : formation of formaldehyde, acetone, campholenealdehyde and pinonaldehyde.

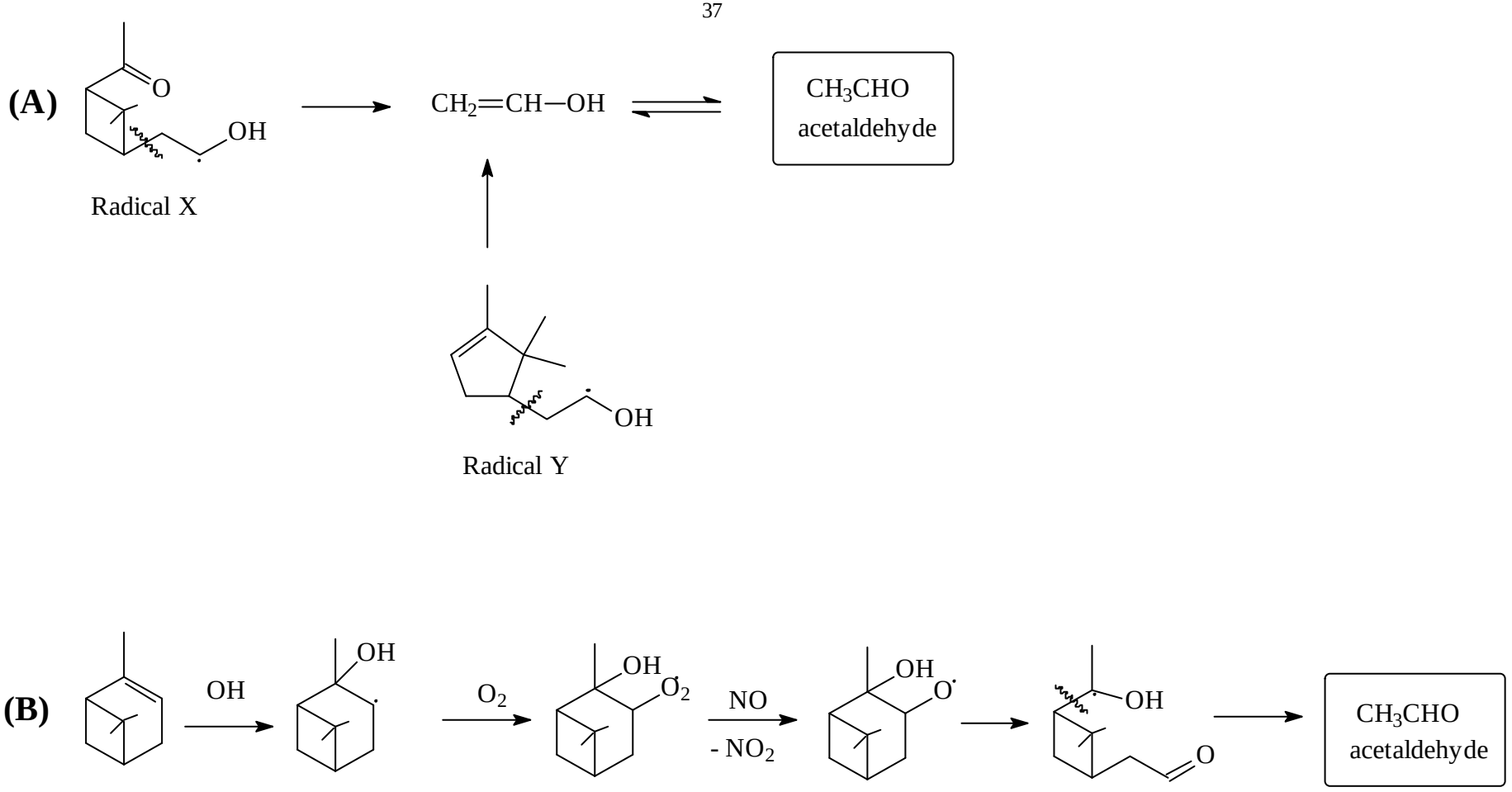

Figure 12 : Mechanism for the reaction between α-pinene and OH : proposed pathways for the formation of acetaldehyde

The presence of pinonaldehyde has been quantified by several research groups [Hatakeyama et al. (1991), Nozière et al. (1999), Arey et al. (1990), Hakola et al. (1994), Pilling et al. (1997)]. It should be pointed out that Nozière et al. (1999) reported a yield for pinonaldehyde of 87 ± 20 %, which is in fairly good agreement with our measurements. The yields of acetone measured in this study (16 ± 1 mole % at 50 Torr and 6 ± 2 mole % at 100 Torr) are of the same order of magnitude as the values found in other studies: 11 ± 2.7 % [Aschmann et al. (1998)], 9 ± 6 % [Nozière et al. (1999)]. The yields of formaldehyde (9.7 ± 0.7 mole % at 50 Torr and 6 ± 5 mole % at 100 Torr) are somewhat smaller than the value (23 ± 9 %) reported by Nozière et al. (1999).

3.5. Discussion and interpretation of laboratory results for b-pinene

From the GC-MS and HPLC-MS analysis, the following oxidation products were identified for the β-pinene/OH reaction : formaldehyde, acetaldehyde, acetone, trans-3-hydroxynopinone, nopinone, perilla alcohol, perillaldehyde and myrtanal. Formaldehyde and nopinone are the most important oxidation products. Plausible reaction paths leading to the formation of formaldehyde, nopinone, perilla alcohol, perillaldehyde, acetone and myrtanal are given in figure 13 to 17. For the other oxidation products a reaction mechanism has still to be designed. In the mechanism for perillaldehyde (figure 17), product A is unstable and in acid medium, this compound will decompose leading to the formation of perillaldehyde.

Up till now only formaldehyde and nopinone have been identified in other studies as oxidation products of the β-pinene/OH reaction. Formaldehyde was also identified by Orlando et al. (2000) and Hatakeyama et al. (1991) but here FT-IR was used. The presence of nopinone was demonstrated by several techniques : GC-MS and GC-FT-IR [Hakola et al. (1994)], GC-MS and GC-flame ionisation detection [Arey et al. (1990)] and FT-IR [Hatakeyama et al. (1991)].

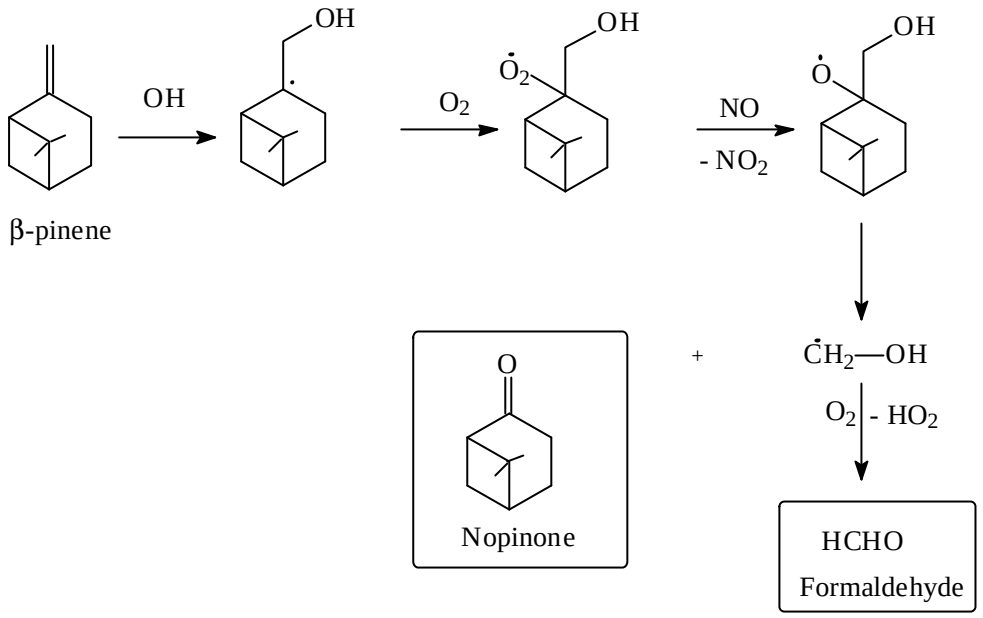

Figure 13 : Mechanism for the reaction between β-pinene and OH : formation of formaldehyde and nopinone

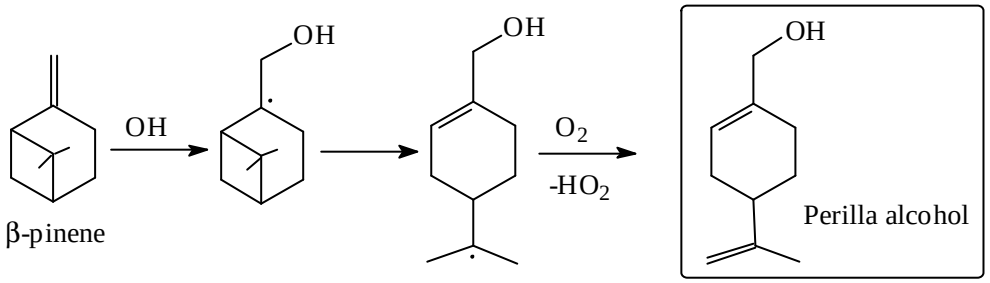

Figure 14 : Mechanism for the reaction between β-pinene and OH : formation of perilla alcohol

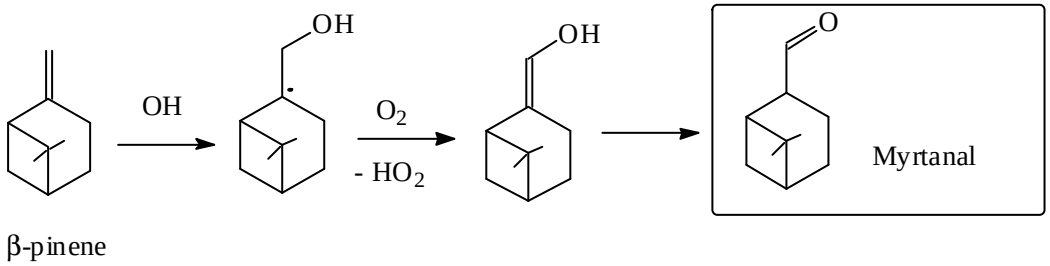

Figure 15 : Mechanism for the reaction between β-pinene and OH : formation of myrtanal

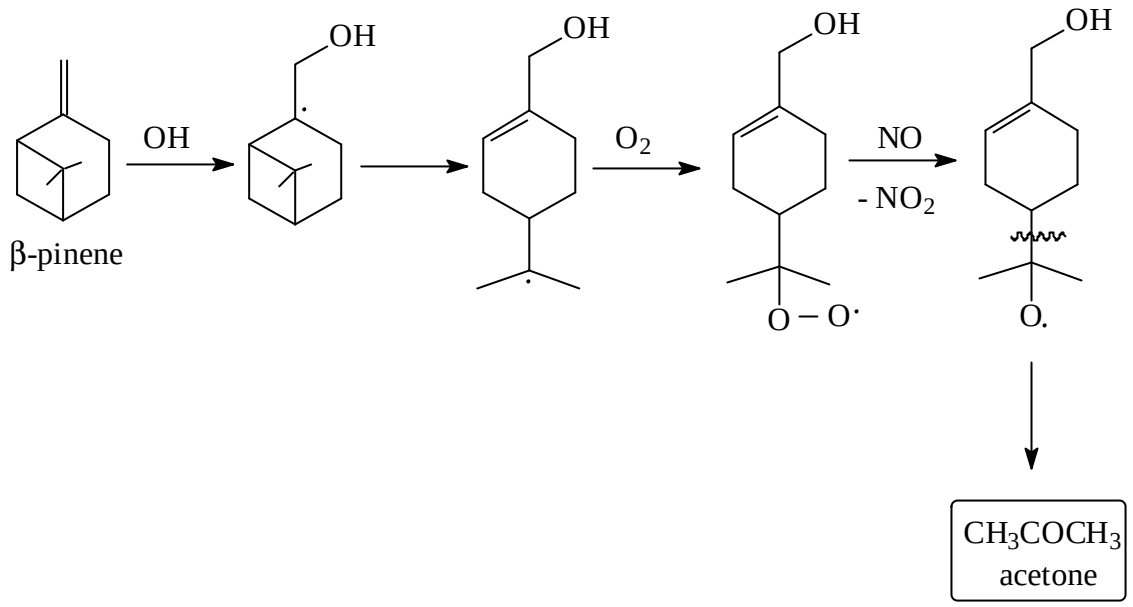

Figure 16 : Mechanism for the reaction between β-pinene and OH : formation of acetone

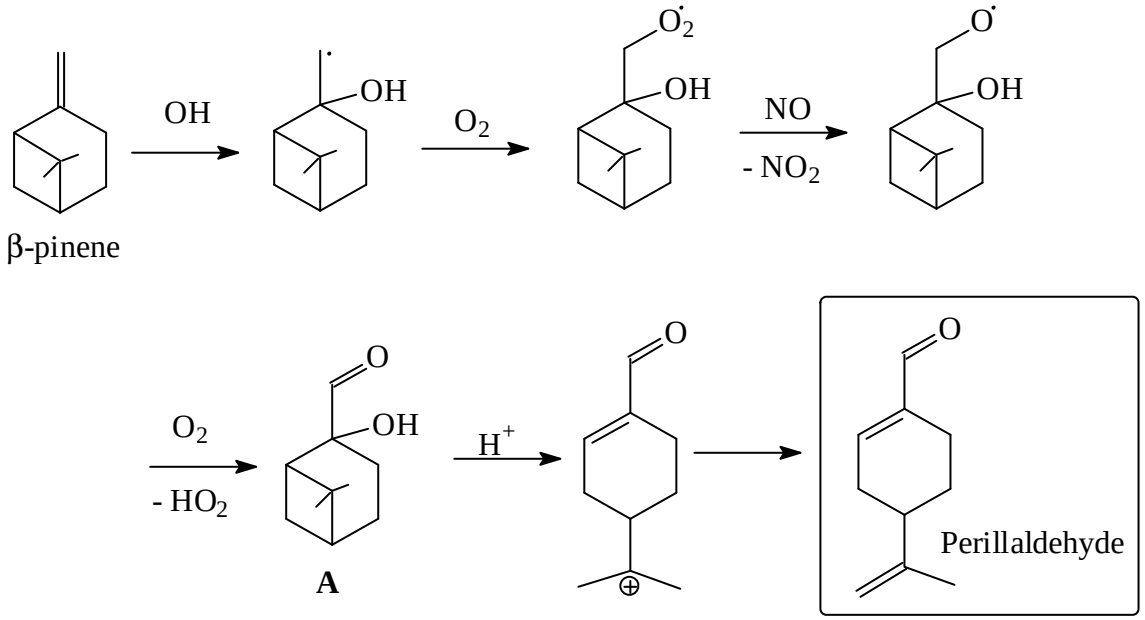

Figure 17 : Mechanism for the reaction between β-pinene and OH : formation of perillaldehyde

3.6. Understanding the photochemical production of ozone in the upper troposphere: quantification of the sources of HO_x and NO_x

As described in section 2.10, the IMAGES model has been used to identify and quantify the sources of HO_x in the upper troposphere (Müller and Brasseur, 1999). Figure 18 displays the relative contribution (in %) of different chemical processes to the total production of HO_x in the UT/LS. As expected, ozone photolysis is found to be dominant in the lower and middle troposphere. The photo-oxidation of acetone is shown to be a large and ubiquitous source of HO_x in the UT/LS, especially in the tropopause region (up to 40%). The other sources are found to be important as well: in particular the photolysis of hydroperoxides over oceanic regions, and the photo-oxidation of aldehydes over continental regions, where anthropogenic as well as biogenic emissions lead to high concentration of such compounds in the PBL. The role of these different sources of HO_x on the production of ozone has also been investigated. For example, we demonstrated that the inclusion of acetone in the model calculations increases by about 20% the calculated impact of subsonic aircraft NO_x emissions on UT/LS ozone.

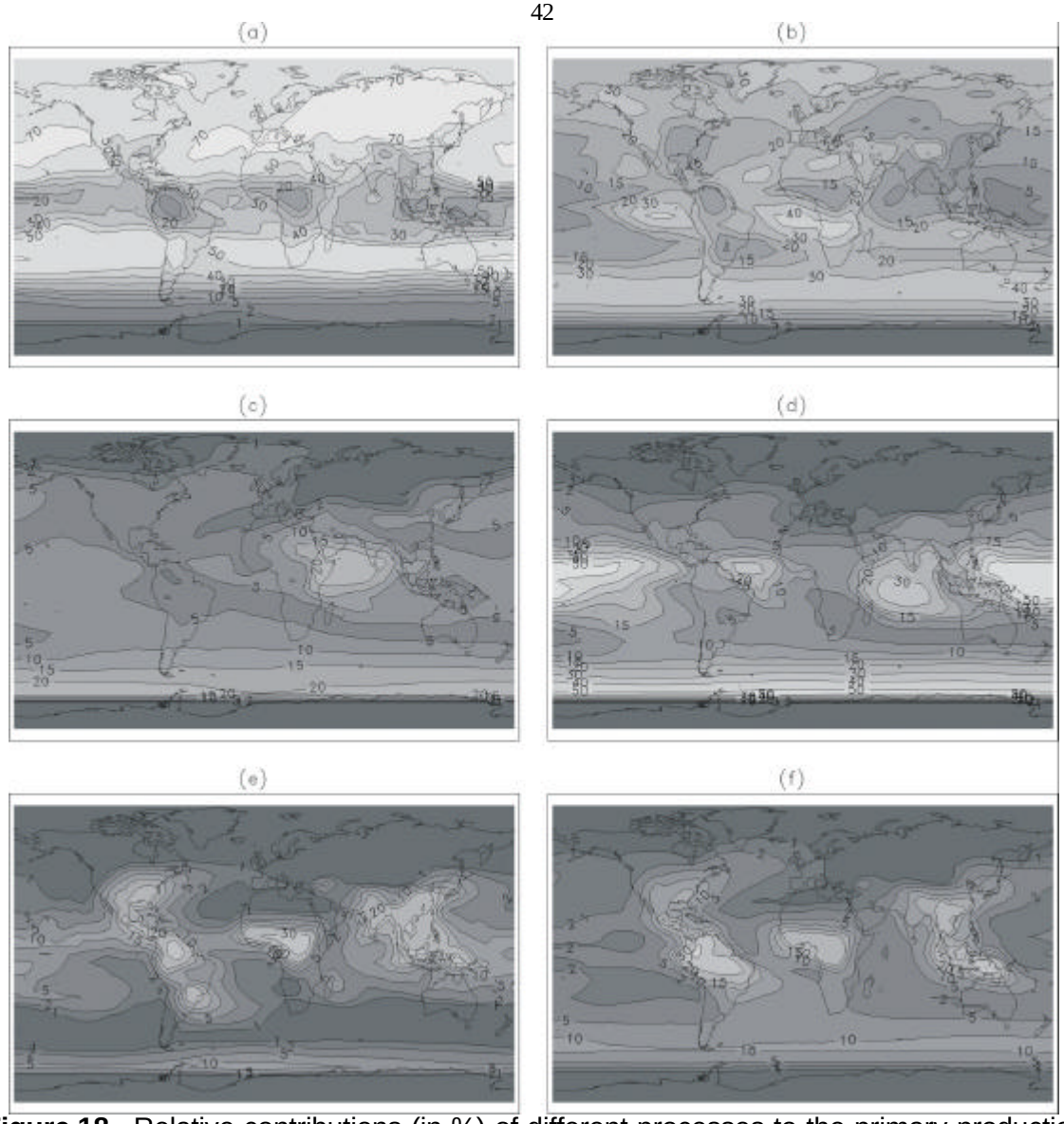

Figure 18. Relative contributions (in %) of different processes to the primary production of HO_x in the upper troposphere (approx. the 240 mb level): (a) ozone photolysis; (b) acetone photooxidation; (c) photolysis of lower tropospheric H_2O_2; (d) photooxidation of lower tropospheric CH_3OOH; (e) photolysis of lower tropospheric CH_2O; (f) photooxidation of C_2 aldehydes. Adapted from Müller and Brasseur (1999).

The "tagging" technique described in section 2.12 allowed the quantification of the contributions of different sources on the NO_x concentrations in this region. For instance, the current aircraft fleet is found to contribute to about 20% of the NO_x levels at the mid-latitude tropopause (Lamarque et al., 1996). This estimate is uncertain, however, because the lightning source is poorly quantified (2-20 Tg (N)/year globally according to recent estimates). We also demonstrated the importance of prescribing realistic vertical profiles of NO production by lightning in tropospheric CTMs, since this profile is found to impact UT/LS NO_x levels by up to 35% (Pickering et al., 1998).

3.7. Modelling the impact of human activities on the global tropospheric composition

The IMAGES model has been used to estimate the past and future changes in the composition of the troposphere resulting from human activities.

The pre-industrial (ca. 1850) composition has been simulated. The results demonstrate that anthropogenic emissions of chemical compounds caused by industrial activities at mid-latitudes in the Northern hemisphere and by biomass burning in the tropics have produced a large increase in the abundance of tropospheric ozone (about a factor of 2 at the surface in the Northern mid-latitudes on zonal average). Industrialization is also found to lead to a reduction in the oxidizing capacity of the atmosphere (globally averaged OH concentration reduced by 17% and methane lifetime enhanced by 1.5 years) (Brasseur et al., 1998). These perturbations in tropospheric ozone result in a change in annually averaged radiative forcing of 0.37 W m^{-2}. The model calculation also show a large increase in the concentrations of sulfur oxides and sulfates since pre-industrial times, amounting to a factor 2-3 on global average, and reaching more than two orders of magnitude at the surface at some locations (Pham et al., 1996).

The calculated wet and dry deposition fields for nitrogen oxides (the NO_y family) predicted by IMAGES and four other global CTMs were used to drive a model for terrestrial carbon uptake (Holland et al., 1997). From this study it is found that global air pollution might have a significant influence on the global carbon cycle. If nitrogen fertilization of the terrestrial biosphere accounts for a substantial portion of the terrestrial "missing" carbon sink, we expect important reductions in its magnitude over the next century as ecosystems become nitrogen saturated and ozone pollution expands.

Future changes in tropospheric ozone associated with a population increase and economic development (primarily in developing countries) are expected to be largest in the tropics, specifically in South and Southeast Asia. Further changes in the oxidizing capacity of the atmosphere could be small if the abundance of tropospheric water vapor increases as a result of anticipated climate change. In the framework of an international cooperation effort (the 3rd IPCC Report), IMAGES and many other models were used to simulate the expected changes in ozone and other compounds in the 21st century.

The possible impact of the current (1992) and future (2015-2050) aircraft fleet has been also evaluated using IMAGES (Brasseur et al., 1996), in part in the framework of the special IPCC assessment on Aviation and the Global Atmosphere.

4. VALORISATION OF RESULTS

- Our results have been made available by communications in international conferences and publications in international journals, as well as e.g. via an EUROTRAC programme website.

- The laboratory results of our project has been incorporated in the European Environmental Research Programme EUROTRAC 2, within the project "Chemical Mechanism Development" (CMD).

- The model results on the future impact of aviation and industrialisation on the tropospheric composition are contribution to two assessment reports of the Intergovernmental Panel for Climate Change (IPCC).

5. CONCLUSIONS : RECOMMENDATIONS

- Given the widely accepted importance of tropospheric chemistry in outstanding issues such as climate change and air quality, and because of the large remaining uncertainties in the processes involved, we strongly recommend that the Belgian and European research efforts be sustained and possibly enhanced in this area.

- More specifically, noting the importance of the biosphere in the climate system as well as the very large remaining uncertainties in the quantification of biospheric emissions and impacts, we recommend that research efforts be sustained in this area.

- The emissions of non-greenhouse gases like carbon monoxide, nitrogen oxides, and non-methane hydrocarbons are known to enhance the abundance of ozone (a greenhouse gas) in the troposphere. These emissions should be considered in future efforts to mitigate climate change.

- Tropospheric ozone levels are expected to increase to very high values in many heavily populated areas of the world, thereby representing a considerable threat to human health and agricultural yields in these areas. We recommend that strategies be elaborated in order to reduce the emissions of ozone precursors (carbon monoxide, nitrogen oxides and hydrocarbons), not only in our countries, but also in the rest of the world.

6. REFERENCES

- Arey, J., Atkinson, R. and Aschmann, S. 1990. Product study of the gas-phase reactions of monoterpenes with the OH radical in the presence of NO_x. J. Geophys. Res. 95 : 18539-18546.
- Aschmann, S.M., Reissell, A., Atkinson, R. A. and Arey, J. 1998. Products of the gas-phase reactions of the OH radical with alpha and beta-pinene in the presence of NO, J. Geophys. Res. 103 : 25553-25561.
- Atkinson, R. and Arey, J. 1998. Atmospheric chemistry of biogenic compounds. Acc. Chem. Res. 31 : 574-583.
- Behforouz, M., Bolan, J. L. and Flyn, M. S. 1985. 2,4-Dinitrophenylhydrazones : A modified method for the preparation of these derivatives and an explanation of previous conflicting results. J. Org. Chem. 50 : 1180-1189.
- Brasseur G., J.-F. Müller, C. Granier, Atmospheric impact of NO_x emissions by subsonic aircraft: A three-dimensional model study, J. Geophys. Res., 101, 1423-1428, 1996.
- Brasseur, G., J. Kiehl, J.-F. Müller, T. Schneider, C. Granier, X.X. Tie, D. Hauglustaine 1998a. Past and future changes in global tropospheric ozone: Impact on radiative forcing. Geophys. Res. Lett. 25 : 3807-3810.
- Brasseur G., D. Hauglustaine, S. Walters, P. Rasch, J.-F. Müller, C. Granier, X. X. Tie 1998b. MOZART: A global chemical transport model for ozone and related chemical tracers, Part1. Model description. J. Geophys. Res. 103 : 28,265-28290.
- Brocheton F., J.-F. Müller, B. Aumont, G. Toupance 2001. On the importance of a detailed chemistry of NMHC in 3D global models. In preparation.
- Carter, W. P. L. and Atkinson, R. 1996. Development and evaluation of a detailled mechanism for the atmospheric reactions of isoprene and NO_x. Int. J. Chem. Kin. 28 : 497-530.
- Chin, M., R. Rood, S.-J. Lin, J.-F. Müller, and A. Thompson 2000. Atmospheric sulfurcycle simulated in the global model GOCART: Model circulation and global properties. J. Geophys. Res. 105 : 24671-24687.
- Clerbaux, C., P. Chazette, J. Hadji-Lazaro, G. Mégie, J.-F. Müller, S. A. Clough 1998. Remote sensing of CO, CH4, and O3 using a space-borne nadir-viewing interferometer, J. Geophys. Res. 103 : 18,999-19,013.
- Emmons, L., D. Hauglustaine, J.-F. Müller, M. A. Carroll, G. Brasseur, D. Brunner, J. Staehelin, V. Thouret, and A. Marenco 2000. J. Geophys. Res. 105 : 20497-20538.
- Fantechi, G. 1999. PH.D thesis, Faculty of Sciences, KULeuven.
- Friedl F., editor, 1997. Atmospheric effects of subsonic aircraft: Interim assessment report of the Advanced Subsonic Technology Program. NASA Reference Publ. 1400, Washington, D.C., 143 pp.
- Granier, C., J.-F. Müller, S. Madronich, and G. Brasseur 1996. Possible causes for the 1990-1993 decrease in the global tropospheric CO abundance: A three-dimensional sensitivity study. Atmos. Environ. 30 : 1673-1682.
- Granier, C., G. Pétron, J.-F. Müller, G. Brasseur 1999. A three-dimensional study of the global CO budget. Chemosphere: Global change science 1 : 255-261.

- Granier, C., G. Pétron, J.-F. Müller, G. Brasseur 2000. The impact of natural and anthropogenic hydrocarbons on the tropospheric budget of carbon monoxide. Atmos. Environ. 34 : 5255-5270.
- Grosjean, D. 1983. Chemical ionization mass spectra of 2,4-dinitrophenylhydrazones of carbonyl and hydroxycarbonyl atmospheric pollutants. Anal. Chem. 55 : 2436-2439.
- Grosjean, D., Williams, E. and Seinfeld, J. 1992. Atmospheric oxidation of selected terpenes and related carbonyls : gas-phase carbonyl products. Env. Sci. Technol. 26 : 1526-1533.
- Grosjean, E. and Grosjean, D. 1995. Liquid chromatographic analysis of C1-C10 carbonyls. Intern. J. Environ. Anal. Chem. 61 : 47-64.
- Grosjean, E., Green, P.G. and Grosjean, D. 1999. Liquid chromatography analysis of carbonyl (2,4-dinitrophenyl)hydrazones with detection by diode array ultraviolet spectroscopy and by atmospheric pressure negative chemical ionization mass spectrometry. Anal. Chem. 71 : 1851-1861.
- Guenther A., Zimmerman P., and Harley P. 1993. Isoprene and Monoterpene emission rate variability: Model evaluations and sensitivity analyses. J. Geophys. Res., 98, 12609-12617.
- Guenther, A., Hewith, C.N., Erickson, D., Fall, R., Geron, C., Graedel, T., Harley, P., Klinger, L., Lerdau, M., McKay, W.A., Pierce, T., Scholes, B., Steinbrecher, R., Tallamraju, R., Taylor, J. and Zimmerman, P. 1995. A global model of natural volatile organic compound emissions. J. Geophys. Res. 100 : 8873-8892.
- Hakola, H., Arey, J., Aschmann, S.M. and Atkinson, R. 1994. Product formation from the gas-phase reactions of OH radicals and O_3 with a series of monoterpenes. J. Atmos. Chem. 18 : 75-102.
- Hanst, P.L., Spence, J.W. and Edney, E.D. 1980. Carbon monoxide production in photooxidation of organic molecules in the air. Atmos. Env. 14 : 1077-1088.
- Hatakeyama, S., Izumi, K., Fukuyama, T., Akimoto, H.1991. Reactions of OH with α-pinene and β-pinene in air : estimate of global CO production from the atmospheric oxidation of terpenes. J. Geophys. Res. 96 : 947-958.
- Hauglustaine D., G. Brasseur, S. Walters, P. J. Rasch, J.-F. Müller, L. K. Emmons, M. A. Carroll 1998. MOZART: A global chemical transport model for ozone and related chemical tracers, Part 2. Model results and evaluation. J. Geophys. Res. 103 : 28,291.
- Hoffmann, T., Odum, J.R., Bowman, F., Collins, D., Klockow, D., Flagan, R.C. and Seinfeld, J. 1997. Formation of organic aerosols form the oxidation of biogenic hyrodcarbons. J. Atmos. Chem. 26 : 189-222.
- Holland E., B. Braswell, J.-F. Lamarque, A. Townsend, J. Sulzman, J.-F. Müller, F. Dentener, G. Brasseur, H. Levy II, J. Penner, G.-J. Roelofs 1997. Variations in the predicted spatial distribution of atmospheric nitrogen deposition and their impact on carbon uptake by terrestrial ecosystems. J. Geophys. Res. 102 : 15849-15866.
- Jay, K. and Stieglitz , L. 1989. Identifizierung chemischer-photochemischer Umsetzungsprodukte van Biogenen Kohlenwasserstoffen mit Antroppgenen Luftschadstoffen. Report KFK-PEF 53, Karlsruhe, 177.
- Kanakidou M., F. J. Dentener, G. Brasseur, T. K. Berntsen, W. Collins, D. Hauglustaine, S. Houweling, I. Isaksen, M. Krol, M. Lawrence, J.-F. Müller, N. Poisson, G. J. Roelofs, Y.

Wang, W. Wauben 1999a. 3-D global simulation of tropospheric CO distributions - results of the GIM/IGAC intercomparison 1997 exercise. Chemosphere: Global Change Science 1 : 263-282.

- Kanakidou, M., F. Dentener, G. Brasseur, W. Collins, T. Berntsen, D. Hauglustaine, S. Houweling, I. Isaksen, M. Krol, K. Law, M. Lawrence, J.-F. Müller, P. Plantevin, N. Poisson, G.-J. Roelofs, Y. Wang, W. Wauben 1999b. 3-D global simulations of tropospheric chemistry with focus on ozone distributions, Report EUR 18842 to the European Union, European Communities.
- Kölliker, S., Oehme, M. and Dye, C. 1998. Structure elucidation of 2,4-dinitrophenylhydrazone derivatives of carbonyl compunds in ambient air by HPLC/MS and multiple MS/MS using Atmospheric Chemical Ionization in the negative ion mode. Anal. Chem. 70 : 1979- 1985.
- Lamarque, J.-F., G. Brasseur, P. Hess, J.-F. Müller 1996. Three-dimensional study of the relative contributions of the different nitrogen sources in the troposphere. J. Geophys. Res. 101 : 22955-22968.
- Lambert, J.-C., J. Granville, M. Van Roozendael, J.-F. Müller, J.-P. Pommereau, F. Goutail, A. Sarkissian 1999. A pseudo-global correlative study of ERS-2 GOME NO2 data with ground-, balloon-, and space-based observations. Proceedings of ESAMS (European Symposium on Atmospheric Measurements from Space '99, ESTEC, Noordwijk, WPP-161, Vol. I : 217-224.
- Lavallée, P. and Bouthillier, G. 1986. Efficient conversion of (1R,5R)-(+)-α-pinene to (1S,5R)-(-)- nopinone. J. Org. Chem. 51 : 1362-1365.
- Law, K., P-H. Plantevin, V. Thouret, A. Marenco, W.A.H. Asman, M. Lawrence, P. Crutzen, J-F. Müller, D. Hauglustaine and M. Kanakidou 2000. Comparison between Global Chemistry Transport Model Results and Measurement of Ozone and Water Vapor by Airbus In-Service Aircraft (MOZAIC) Data. J. Geophys. Res. 105 : 1503-1525.
- Lee, J., S.C. Doney, G. Brasseur, J.-F. Müller 1998. A global 3-D coupled atmospheric-oceanic model of methyl bromide, J. Geophys. Res. 103 : 16,039-16,057.
- Müller, J. F. 1992. Geographical distribution and seasonal variation of surface emissions and deposition velocities of atmospheric trace gasses. J. Geophys. Res. 97 : 3787-3804.
- Müller, J. F. and Brasseur, G. 1995. Images – A 3-dimensional chemical transport model of the global troposphere. J. Geophys. Res. 100 : 16445-16490.
- Müller, J. F. and Brasseur, G. 1999. Sources of upper tropospheric HOx: A three-dimensional study. J. Geophys. Res. 104 : 1705-1715.
- Nozière, B., Barnes, I. and Becker, K.H. 1999. Product study and mechanisms of the reactions of α-pinene and pinonaldehyde with OH radicals. J. Geophys. Res. 104 : 23645-23656.
- Peterson, P.E. and Grant, G. 1991. Preparation of chiral inducers having the bicyclo [3.1.1.] heptane framework. Assignement of diastereomer configuration by NMR and comparison of calculated and observed coupling constants. J. Org. Chem. 56 : 16-20.
- Pétron, G., Granier C., Khattatov B., Lamarque J.-F., Yudin V., Müller J.-F., Gille J. 2001. Inverse modeling of carbon monoxide surface emissions using NOAA-CMDL network observations. Submitted to J. Geophys. Res.

- Pham, M., J.-F. Müller, G. Brasseur, C. Granier, and G. Mégie 1995. A three-dimensional study of the tropospheric sulfur cycle. J. Geophys. Res. 100 : 26061-26092.
- Pham, M., J.-F. Müller, G. Brasseur, C. Granier, and G. Mégie 1996. A 3D model study of the global sulphur cycle: contributions of anthropogenic and biogenic sources. Atmos. Environ. 30 : 1815-1822.
- Pickering, K. E., Y. Wang, W.-K. Tao, C. Price, J.-F. Müller, Vertical distributions of lightning NOx for use in regional and global chemical transport models 1999. Atmos. Environ. 33 : 1403-1422.
- Pilling, M., Saunders, S., Carslaw, N., Pascoe, S., Jenkin, M. and Derwent, D. 1999. http://cast.nerc.ac.uk/LIBRARY/MCM2/html/main.html
- Pötter, W. and Karst, U. 1996. Identification of chemical interferences in aldehyde and ketone determination using dual-wavelength detection. Anal. Chem. 68 : 3354-3358.
- Orlando, J. J., Nozière, B., Tyndall, G. S. Orzechowska, G. E., Paulson, S. E. and Rudich, Y. 2000. Product studies of the OH- and ozone-initiated oxidation of some monoterpenes. J. of Geophys. Res. 105 : 11561-11572.
- Stenhagen, E. and Abrahamsson, S. 1968. Registry of Mass Spectral Data. F.W. McLafferty, Wiley, New York.
- Thakur, A., H. Singh, P. Mariani, Y. Chen, Y. Wang, D. Jacob, G. Brasseur, J.-F. Müller, M. Lawrence 1999. Distribution of reactive nitrogen species in the remote free troposphere: Data and model comparisons, Atmos. Environ 33 : 1403-1422.
- Vairavamurthy, A., Roberts, J.M. and Newman, L. 1992. Methods for the determination of low molecular weight carbonyl compounds in the atmosphere : a review. Atmos. Environ. 26A : 1965-1993.
- Van den Bergh, V., Vanhees, I., De Boer, R., Compernolle, F. and Vinckier, C. 2000. Identification of the oxidation products of the reaction between α-pinene and hydroxyl radicals by gas and high-performance liquid chromatography with mass spectrometric detection. J. of Chromat. A. 896: 135-148.
- Van den Bergh, V. Coeckelberghs, H., Vanhees, I., De Boer, R., Compernolle, F. and Vinckier, C. 2001. Determination of the oxidation products of the reaction between α,β-pinene and OH-radicals by HPLC-MS. Analytical and Bioanalytical Chemistry, in preparation.
- Vanhees, I., Van den Bergh, V., Schildermans, R., De Boer, R., Compernolle F. and C. Vinckier. 2001. Determination of the oxidation products of the reaction between α-pinene and hydroxyl radicals by high-performance liquid chromatography. J. Chromat. A. 915: 75-83.
- Vereecken, L. and Peeters, J. 2000. Theoretical study of the formation of acetone in the OH-initiated atmospheric oxidation of α-pinene. J. Phys. Chem. A. 104 : 11140-11146.
- Vinckier, C. and Van Hoof, N. 1993. Determination of the sticking coefficient of α-pinene on quartz. Proceedings Eurotrac Symposium, SPB Academic Publ., The Hague, The Netherlands, 652-654.
- Vinckier, C. and Van Hoof, N. 1994. Rate constant of the α-pinene + atomic hydrogen reaction at 295 K. Int. J. Chem. Kin. 26 : 527-534.
- Vinckier, C., Compernolle, F. and Saleh, A.M. 1997. Qualitative determination of the non-volatile reaction products of the α-pinene reaction with hydroxyl radicals. Bull. Soc. Chim. Belg. 106 : 501 – 513.

- Vinckier, C., Compernolle, F., Saleh, A.M., Van Hoof, N. and Vanhees I. 1998. Product yields of the α-pinene reaction with hydroxyl radicals and the implication on the global emission of trace compounds in the atmosphere. Fresenius Environ. Bull. 7: 361-368.
- Warneck, P. 1988. Chemistry of the Natural Atmosphere, Academic Press, San Diego, 158-170.
- Went, F.W. 1960. Blue haze in the atmosphere. Nature 167 : 641-643.
- Yacoub, Y. 1999. Method procedures for sampling aldehyde and ketone using 2,4-dinitrophenylhydrazine – a review. Proc Instn Mech Engrs 213 : 503-517.
- Zhang, S.H., Shaw, M., Seinfeld, J. and Flagan, C. 1992. Photochemical aerosol formation from α-pinene and β-pinene. J. Geophys. Res. 97 : 20717-20729.
- Zimmerman, P.R., Chatfield, R.B., Fishman, J., Crutzen, P. and Hanst, P.L. 1978. Estimates on production of CO and H_2 from oxidation of hydrocarbons on emision from vegetation. Geophys. Res. Lett. 5 : 679-682.